A STUDY OF THE HARDENING MECHANISMS AND MICROSTRUCTURAL CHARACTERISTICS OF AN IMPROVED DENTAL AMALGAM

A Dissertation

Presented to

the Faculty of the Graduate School

University of Missouri - Columbia

In Partial Fulfillment

of the Requirements for the Degree

Doctor of Philosophy

---

by

John William Holland

December, 1975

The undersigned, appointed by the Dean of the Graduate Facul

examined a thesis entitled

A STUDY OF THE HARDENING
MECHANISMS AND MICROSTRUCTURAL CHARACTERISTICS
OF AN IMPROVED DENTAL AMALGAM

presented by John William Holland

a candidate for the degree of Doctor of Philosophy

and hereby certify that in their opinion it is worthy of acceptance.

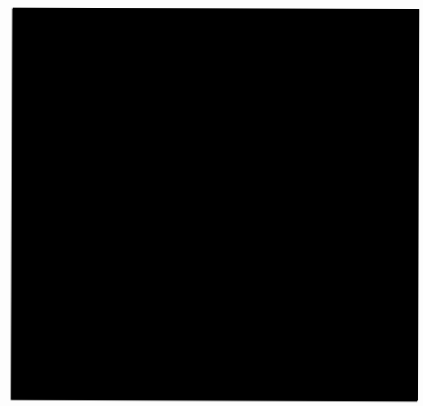

VITA

John Holland was born [redacted] in Union Star, Missouri. After attending public schools in Missouri, he received the following degrees: B.S. in Physics and Mathematics from Central Missouri State University at Warrensburg, Missouri (1970); M.S. in Mechanical Engineering from the University of Missouri at Columbia (1972); Ph.D. in Mechanical Engineering from the University of Missouri at Columbia (1975). Married to the former Elizabeth Young of Union Star, Missouri, he is presently a scientist at Argonne National Laboratory, Argonne, Illinois.

A STUDY OF THE HARDENING MECHANISMS AND MICROSTRUCTURAL CHARACTERISTICS OF AN IMPROVED DENTAL AMALGAM

John William Holland

David A. Hansen Dissertation Supervisor

ABSTRACT

Dispersalloy dental amalgam has been developed in the last twelve years and displays a significant decrease in creep rate and an increased resistance to corrosion. The manufacturer claims that the decreased creep rate results from a dispersion hardening mechanism employed in this radically new amalgam. The product consists of a spherical copper-silver eutectic phase added to a fine-cut amalgam alloy. The ratio of eutectic spheres to fine-cut alloy is approximately 1:2 by weight. Unlike other dispersion hardened alloy systems however, Dispersalloy's tensile strength is somewhat less than for many fine-cut amalgams.

All mechanical and microstructural testing indicates that the system is solution hardened by a distributed copper concentration within the γ_1 matrix phase. Analysis determined that a 3-5 weight percent copper concentration in the Ag_3Sn particles is the source of the copper solute atoms.

In addition, the copper-silver eutectic spheres, present in the amalgam microstructure, act as sinks to tin atoms liberated by the Ag_3Sn-mercury reaction initiated during trituration (mixing). Formation

of a tin-rich shell about the eutectic spheres is beneficial because the tin is then unable to form the deleterious γ_2 phase. It is this phase which is most corrosive and leads to early failure of the amalgam restoration.

Finally, particles observed by some dental researchers upon the polished copper-silver spheres, within the amalgam microstructure, were confirmed to be the result of polishing contamination. The particles are not inherent to the Dispersalloy metallurgy.

TABLE OF CONTENTS

ACKNOWLEDGMENTS

The author is sincerely grateful for the guidance and counseling provided by Dr. David A. Hansen. His assistance was appreciated in many ways.

Dr. Glen Himmelberg is thanked for providing use of the electron microprobe analyzer. The electron microprobe was purchased with funds jointly provided by NSF grant GA 18445 and by the University of Missouri-Columbia.

Dr. Merton Brown performed some of the scanning electron microscopy in this study; his contributions are gratefully acknowledged.

Dr. Carl Johnson and Argonne National Laboratory of Argonne, Illinois, are thanked for informative consultation and monetary assistance.

LIST OF TABLES

LIST OF ILLUSTRATIONS

A STUDY OF THE HARDENING MECHANISMS AND MICROSTRUCTURAL CHARACTERISTICS OF AN IMPROVED DENTAL AMALGAM

CHAPTER I

INTRODUCTION

A significant portion of dental research undertaken in this century has been devoted to characterizing the mechanical and physical properties of dental amalgam. The ultimate goal of this research has been to develop an improved restorative material.

Unquestionably, these research endeavors have been responsible for the improved clinical behavior of dental amalgam. However, a significant fraction of amalgam restorations still fail. A clinical investigation (Moore and Stewart, 1967) of dental restorations had indicated that 42% of the amalgam restorations studied were defective in some manner. Twenty-six percent of all the restorations examined had fractured in service. Another study (Seino, 1966) reported that as many as 32% of the amalgam restorations had fractured, out of the total number of cases studied.

Historically, research efforts to decrease the fracture incidence of dental amalgam were assessed in terms of an increase in the compressive strength of the amalgam material. It was widely believed that only compressive stresses existed in the restoration during mastication. Modern analysis of clinical and laboratory data indicates that many restorations fail from the seemingly inherent weakness of the amalgam under tensile stress. "Shock" loading and tensile stress have been shown to initiate fracture of dental amalgams (Jorgenson, 1965; Mahler, 1958).

During mastication, the amalgam is externally loaded by compressive forces. At the amalgam-tooth interface, the amalgam margin can be considered a geometric wedge. This situation is illustrated in Figure 1.

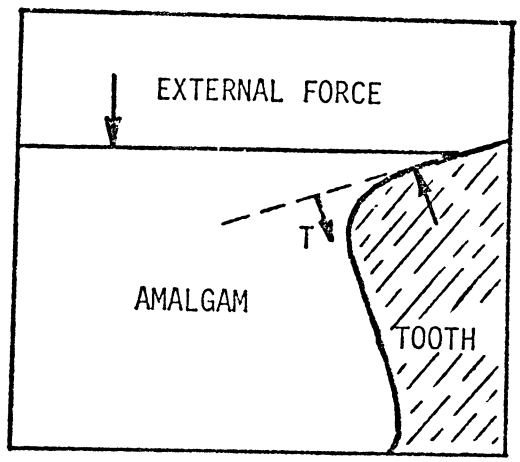

Figure 1. Loading of Dental Amalgam for Marginal Fracture

Loading of the amalgam induces tensile stresses (T) within the marginal wedge. One such orientation of the tensile stresses is illustrated in the above figure. Other tensile stress distributions in this system are analagous to the stress distribution in the cross section of a transversely loaded cantilever beam.

A 10:1 compressive strength to tensile strength ratio has been reported by Young and Johnson (1967). Since materials may fail by a shear mechanism when the stresses are compressive, the shear strength of amalgam also is much larger than its tensile fracture strength. Experimentally, amalgam characteristically fractures prior to exceeding the shear strength of the material. Hence, the tensile fracture strength assumes a dominant role in determining the failure mode of amalgam.

A number of investigators have shown the fracture mode of dental amalgam to be typically brittle (Jorgenson, 1965; Asgar and Sutfin,

1965; Young and Johnson, 1967). Brittle materials exhibit fracture with little or no macroscopic evidence of local plastic deformation.

Although amalgam behaves like a "brittle" material under the high rates of load application common to the masticatory process, certain physical property tests demonstrate a propensity for creep (Mahler and Van Eysden, 1969). Creep is the progressive time-dependent deformation of a material at constrant stress level less than the yield or fracture stress. Mahler et al. in another study (Mahler, Terkla, Van Eysden and Reisbick, 1970) demonstrated that the rheological properties of high dynamic creep, high static creep and low slow compressive strength do appear to correlate with marginal fracture.

There exists clear evidence, from both clinical and laboratory studies, that corrosion is also an important contributing factor to amalgam fracture. The combined results of work by Burdekin and Gibbs (1972), Guthraw et al. (1967), Jorgenson and Saito (1970), Marek and Hochman (1973), Marek et al. (1973), Mateer and Reitz (1970, 1972), Stoner et al. (1971) and others, have lead to a general understanding of the corrosion process in silver-tin amalgam. It appears that conventional Ag-Sn amalgam corrosion is primarily an attack on the tin rich γ_2 (Sn_{7-8} Hg) phase in amalgam. The evidence clearly suggests that γ_2 exists as an interconnected framework through γ_1 (Ag_2 Hg_3) and unreacted γ(Ag_3 Sn) phases (Mateer and Reitz, 1970, 1972; Jorgenson and Saito, 1970). As the γ_2 phase is destroyed by corrosion, the framework disappears, and the remaining matrix of γ_1 and γ_2 is correspondingly weakened.

Limited corrosion at the margin is probably beneficial in that the corrosion products appear to seal the margin and thereby prevent

seepage of oral fluids through the margin (Wagner, 1972). However, clinical data indicate that continuous margin corrosion can occur, leading to a gross weakening of the amalgam margin (e.g., Mateer and Reitz, 1970). Again, this corrosion is indicated as involving the destruction of the γ_2 framework structure.

Numerous independent studies have confirmed that at least three property-related mechanisms can lead to the early fracture of dental amalgam restorations. The correlating properties are low tensile strength, high creep rate and a susceptibility for corrosion. In light of the previous findings cited, it would seem that all three mechanisms combine synergistically to degrade the amalgam, leading to early margin failure. In support, Paffenbarger (1966) has suggested that phase changes, mercuroscopic expansion, corrosion, creep and thermal expansion are inter-related in the extrusion and eventual margin fracture of amalgam.

Mercuroscopic expansion is a result of corrosion at the amalgam margin. Mercury is released during corrosive attack, and it penetrates the amalgam surface to react with the retained $\gamma(Ag_3\ Sn)$ phase. γ_1 ($Ag_2\ Hg_3$) grains are formed from this reaction; the formation of these γ_1 grains causes a local volume expansion termed mercuroscopic expansion.

Wilkinson and Haack (1958) hypothesized that the early failure of amalgam restorations could be explained by the material's low fatigue strength. The early failure of a material can be caused by repeated loading if the stress is repeated a sufficient number of times; the maximum repeated stress might be considerably less than the fracture strength of the material. A failure induced in this manner is called a fatigue failure. Few additional fatigue investigations were performed;

it is now thought that amalgam's low fatigue strength is of secondary importance in explaining the early failure of amalgam.

The synergistic combination of low tensile strength, high creep rate, a susceptibility for corrosion and related phenomena (e.g. mercuroscopic expansion) can possible lead to early amalgam failure in the following manner:

(1) Weakening of the marginal shelf and adjacent support material by corrosive attack,

(2) Extension of the cantilevered margin as a result of creep under masticatory loading and mercuroscopic expansion,

(3) Fracture of the amalgam margin resulting from the induced tensile stresses exceeding the fracture strength of the amalgam material.

It should be emphasized for dental amalgam, as for many engineering materials, that the ultimate fracture event of the component is not uniquely the result of a single cause. As for amalgam, all three rheological properties stated earlier are major contributors to the final fracture of amalgam restorations.

By improving the three rheological properties of amalgam stated earlier, manufacturer's and dental clinicians have made significant advances in decreasing the early failure of amalgam restorations.

In early investigations, the amalgam properties were altered by changing the manipulative variables. These variables included trituration (mixing) technique and time, amalgam handling technique, compaction pressure, etc. Only limited success resulted from these studies.

The clinical dentist, although responsible for the integrity of the restoration, has secondary control over the quality of the amalgam.

It is his responsibility to select the proper restorative material for a particular restoration type. When the use of dental amalgam is indicated, it is the dentist's additional responsibility to select the best amalgam, based upon laboratory and clinical evidence, currently being marketed. He must provide for proper cavity design and preparation, correct amalgam mixing and handling technique, and apply adequate compaction pressure to the plastic amalgam mass in the cavity.

The amalgam manufacturer must provide a high quality amalgam before a dentist can prepare a more fracture resistant restoration. Traditionally, dental amalgam manufacturers have varied the alloy composition slightly to afford changes in bulk corrosion resistance, mercuroscopic expansion and setting times, among others. More profound changes were produced by altering the mercury to alloy ratio which directly results in changes in compressive strength, tensile strength, mercuroscopic expansion and setting time (Paffenbarger, 1966).

The use of spherical alloy particles instead of irregularly-shaped, lathe-cut alloy particles leads to quite different amalgam properties. When an amalgam consisting of both spherical and lathe-cut alloy particles is used further improvement of strength and creep properties is observed (Mahler et al., 1970).

About twelve years ago, an amalgam alloy exhibiting a significant departure from traditional alloys was introduced in Canada (Innes and Youdelis, 1963). This product consisted of a spherical, silver-copper eutectic phase added to a conventional fine-cut amalgam. The ratio of spherical eutectic phase to fine-cut alloy was 1:2 by weight. The rationale for this innovation was to effect an increase in strength and a decrease in creep rate by a dispersion hardening mechanism.

Dispersalloy* is the marketed amalgam which utilizes the dispersion hardening mechanism suggested by Innes and Youdelis (1963). Mahler et al. (1970) compared the compressive strength, tensile strength, creep rate and other mechanical properties of Dispersalloy with a fine-cut alloy, New True Dentalloy.** Table 1 indicates the variation of some selected mechanical properties which resulted from the addition of the copper-silver eutectic spheres to a traditional fine-cut alloy.

TABLE 1

Comparison of Alloy Mechanical Properties

Mechanical Property	Dispersalloy	New True Dentalloy
Compressive Strength (psi)	61,400	59,500
Tensile Strength (psi)	6,940	7,930
Creep (%)	0.76	2.36

Greener and Sarkar (1971) determined that Dispersalloy is corrosion resistant, and in fact, corrosion of clinical restorations produced from Dispersalloy could not be detected.

Therefore, it is evident that the low creep rate and corrosion resistance of amalgam were improved with the use of the dispersed copper-silver phase in Dispersalloy. A significant decrease in tensile strength, however, was observed.

*Western Metallurgical Ltd., Edmonton, Saskatchewan, Canada.

** S. S. White Company, Philadelphia, PA, USA.

In more recent studies (Young and Wilsdorf, 1972; Hansen, Holland, Lewis and Moore, 1974), researchers have endeavored to alter mechanical properties of dental amalgam by utilizing metallurgical techniques employed in the production of high strength materials for use in aircraft and other strength critical components.

Young and Wilsdorf (1972) investigated the effect of oxide impurities on the fracture of dental amalgams. The alloy was cleaned in an acid wash to remove the oxide coating which results from oxidation during manufacture and storage. Test specimens prepared from the "cleaned" alloy exhibited an increased tensile strength and an altered fracture mode. The fracture mode in amalgams has been reported to be intergranular (i.e., the crack progresses along grain boundaries) (Asgar and Sutfin, 1965; Young and Wilsdorf, 1972). The amalgam prepared from the "cleaned" alloy exhibited transgranular failure (i.e., the crack through the grains of the amalgam).

Other causes of embrittlement of amalgam were possible and had been observed in various alloy systems. In cast iron and other multiphase alloys, the presence of interstitial elements such as hydrogen or oxygen reduced the tensile strength of those materials. Other systems, such as sulfur in steel, were known to form a weakening grain boundary phase which, at high temperatures, embrittled steel. Trace quantities of substitutional impurities, found in other alloys, resulted in similar effects.

Young and Wilsdorf (1972) demonstrated that interstitial elements were present in dental amalgam alloys (Ag-Sn) as an oxide coating and perhaps as bulk impurities. Asgar and Sutfin (1965) speculated

that impurities segregated at grain boundaries in amalgams could be the dominant factor in determining the properties of the Ag-Sn alloy.

Therefore, it came as no surprise that the study by Hansen et al. (1974) was able to increase the tensile strength of amalgam by eliminating air-borne impurities present during the mixing of the amalgam. The increase in strength was obtained by evacuating the capsule which contained the Ag-Sn alloy and mercury in separate compartments. The capsule was refilled with argon, an inert gas, and it was sealed until the prescribed mixing was complete. Increases in strength up to 11% were attained by this method. Later analysis indicated that the amalgam was also more corrosion resistant following the inert gas treatment (Marek, 1974). However, the creep measurement described by Mahler (1969) indicated that the creep rate remained unchanged at a value typical of other fine-cut alloys.

When considering the more recently used metallurgical techniques to improve the rheological properties of amalgam, the least understood is that used to develop Dispersalloy. Preliminary considerations revealed conflicts between the manufacturer's proposed hardening mechanism and that hypothesized from a consideration of traditionally accepted relationships among mechanical properties and hardening mechanisms. A dispersion hardened system is generally defined as one containing a finely divided, dispersed phase within a matrix phase of a different material. The purpose of the dispersed particles is to act as barriers to dislocation movement; therefore, the dislocation movement is inhibited. At the same time,however, grain boundary cohesion must be maintained at the dispersed phase-matrix interface. The size of the dispersed particles (Cu-Ag eutectic spheres) in Dispersalloy are of the same order as the irregularly-shaped, retained Ag_3Sn, in both

Dispersalloy and in fine-cut alloys. It should therefore be expected that amalgam is already dispersion hardened prior to the addition of the eutectic spheres if, in fact, Dispersalloy is truly a dispersion hardened system.

In engineering materials, dispersion hardening normally results in both increased tensile strength and decreased low temperature creep. However, mechanical testing displayed a decreased creep rate and a decreased tensile strength for Dispersalloy.

Typically for amalgam, low tensile strength is a result of grain boundary weakening. In addition, grain boundary cohesion is essential for dispersion hardening to exist; if otherwise, the localized strain fields cannot be established. Therefore if dispersion hardening exists in Dispersalloy, the grain boundary cohesion required to harden the grain should also result in a higher tensile strength.

Creep of amalgam restoration within the oral cavity is considered low temperature creep since it occurs at a temperature much lower than one-half the alloy absolute melting temperature. Deformation during creep in this temperature range, for engineering materials, has been determined to be solely a result of deformation within the grain (i.e., no grain boundary shear).

It is therefore hypothesized that the manufacturer had made some other alloy addition to the amalgam components which has hardened the Ag_2Hg_3 matrix phase resulting in a decreased creep rate. The addition of the copper-silver spheres contributed to poor grain boundary cohesion; hence the tensile strength of Dispersalloy was reduced since that property in dental amalgams is directly related to the strength of the grain boundaries.

Many questions concerning Dispersalloy remain unanswered by researchers (e.g. the creep hardening mechanism, the explanation of the material's corrosion resistance, and the evaluation of the time-dependent behavior of the alloy). The purpose of this investigation was to gain answers to these questions.

Preliminary studies were designed to determine the creep mode of Dispersalloy and to identify the hardening mechanism of the system. Electron microprobe analysis was performed on the material system to characterize the phase distribution and compositions. In addition, the microstructure was studied in the hope of obtaining an explanation for the unusual electrochemical behavior of Dispersalloy. Mechanical tests were performed on Dispersalloy specimens, of differing ages, in order to determine the variation of tensile strength and creep rate with time. Time studies were also performed on the electron microprobe analyzer to possibly determine the reasons for variations in the mechanical property behavior of the system. Further, the diffusion of elements within the non-equilibrium Dispersalloy microstructure were traced in the microprobe time study.

CHAPTER II

EXPERIMENTAL PROCEDURES

General

The purpose of this chapter is to describe the specimen preparation used in all of the experimental tests, to describe the procedures used in the mechanical testing of the amalgam and to describe the metallographic polishing regime employed in the microanalysis of Dispersalloy. Specific, detailed descriptions of the testing equipment and the associated theories of operation are included in the Appendices of this dissertation.

As in most material research projects, the experimental work was divided into three functional areas: specimen preparation, specimen testing and data analysis. Fortunately, one specimen geometry could be used for all the testing procedures. Specimen testing included both mechanical and microstructural analyses. The diametral compression test, a test specified by the American Dental Association Specification No. 1 (Guide to Dental Materials and Devices, 5th ed., 1970) to determine the amalgam tensile strength, and a static creep test described by Mahler (1969) were used to evaluate those two important mechanical properties of dental amalgam. Electron microbeam analysis was employed to determine phase concentrations, phase distributions and other chemical analyses. The scanning electron microscope aided in the study of microstructural polishing effects and fracture surface analysis.

Due to the many manipulative variables and to the nature of the investigation, special care was required in the specimen preparations

and in the handling of the finished specimen. Strict reproduction of the manipulative variables and a high degree of cleanliness were of prime concern. Since the purpose of the study was to evaluate some of the mechanical and physical properties of Dispersalloy amalgam, the manufacturer's prescribed mixing and handling techniques were followed precisely.

Amalgam Preparation

Alloy

It was not the intent of this research program to demonstrate the superiority of one manufacturer's product over other amalgam brands or types, nor was it the purpose to maximize strengths or optimize properties of one particular amalgam brand. Only Dispersalloy amalgam was investigated in order to determine the reasons for its superior properties.

Predosed, double spill Dispersalloy capsules were used for experimentation; this was done in order to minimize contamination and measuring problems, which often result when bulk components are used in specimen preparation. Figure 2 shows the assembled capsule on the right and the disassembled components comprising the capsule on the left.

The lower portion of the capsule contains a premeasured quantity of powdered alloy and a metal pestle to facilitate mixing; a predosed volume of mercury is sealed within the upper portion of the capsule. This product consists of a silver-copper eutectic phase added to a conventional fine-cut amalgam alloy. The ratio of eutectic phase to conventional alloy is approximately 1:2 by weight.

Figure 2. Dispersalloy Predosed Amalgam Capsule

The amalgam is prepared by admixing the mercury with the alloy and by being intimately mixed together (triturated) with a high speed mechanical Silamat amalgamator* oscillating at approximately 4570 rpm.

Specimen Preparation

The American Dental Association describes in detail the dimension and preparation technique for a standard test specimen in the ADA Specification No. 1 (Guide to Dental Materials and Devices, 5th ed., 1970). This specimen may be used for the diametral compression test, the static creep test and for all microstructural analysis.

*Justi Silamat, A. Williams Justi Ivoclar Product; Liechtenstein.

Equipment used for the ADA preparation include a die and plunger set (see Figures 3 and 4), a static, dead weight press capable of developing 2030 psi pressure on the plastic amalgam mass, an electric timer, a Silamat amalgamator, a Teflon funnel and plunger, rubber-tipped tweezers and cleaning supplies. Illustrated in Figure 5 is the equipment utilized in preparing an ADA specimen.

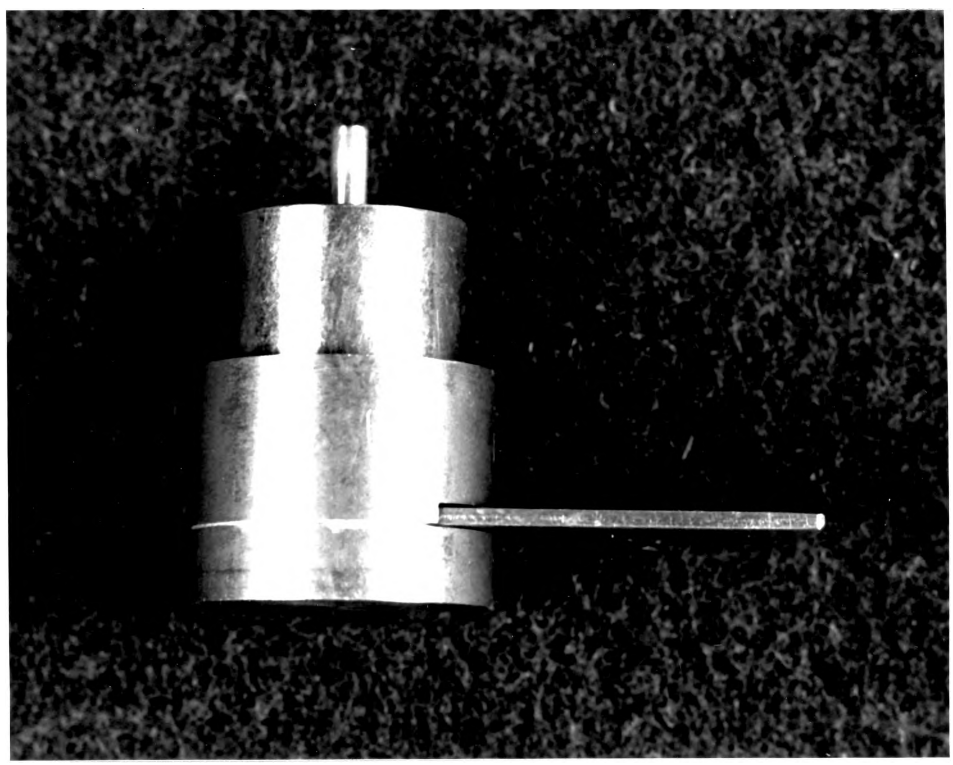

Figure 3. Assembled ADA Standard Die Set

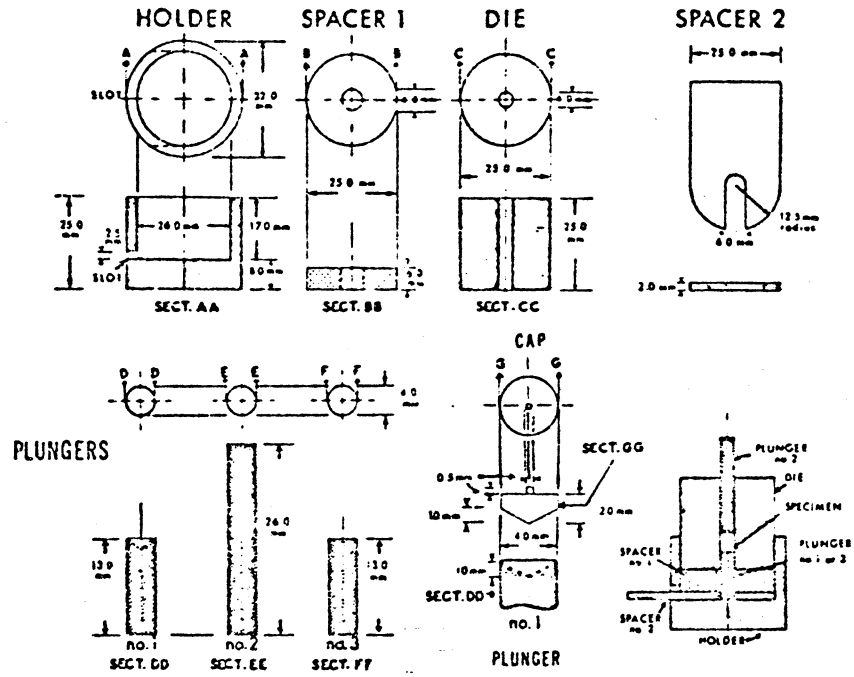

Fig. 1-1 Mold for dental amalgam specimens. Holder, spacers, and cap shall be made of cold rolled steel or no. 303 stainless steel. Die and plungers shall be made of hardened tool steel or 440 C stainless steel. The cap and no. 1 plunger are used when the dimensional change specimens are measured in an interferometer. Working surfaces of die and plungers shall be honed surfaces. Limits of clearance for die and plungers shall be 12 to 25 μ.

Figure 4. ADA Dies (reprinted from the ADA Specifications for Dental Materials)(Guide to Dental Materials and Devices).

Figure 5. Specimen Preparation Equipment

The static press employed uses a lead weight mounted on a lever arm to supply 39.6 pounds to the plunger of the ADA die set (2030 psi pressure on a 4mm diameter plunger). The load is raised or lowered by a lever mounted on a cam. A more detailed description of the static press can be found elsewhere (Holland, 1972). The electric timer was started following the trituration (mixing) sequence in the amalgamator. The Teflon funnel and plunger were employed to facilitate the introduction of the amalgam to the die cavity. Due to the semi-plasticity

of the amalgam specimen immediately after preparation, rubber-tipped tweezers were used to handle the specimen.

TABLE 2

Schedule for Preparation of ADA Specimens

a.	End of trituration (see Figure 6-a)	00 sec.
b.	Place triturated mass in mold and apply 2030 psi pressure (see Figures 6-b,c,d)	30 sec.
c.	Release load and remove no. 2 spacerat (see Figure 6-e)	45 sec.
d.	Replace load at	50 sec.
e.	Release load at	90 sec.
f.	Brush away mercury and eject specimen at (see Figure 6-f)	120 sec.

The amalgam content of one Dispersalloy capsule produced a cylindrical specimen 4mm in diameter by approximately 8.5 mm in length. The room temperature, during preparation, was maintained at 75±2°F; the relative humidity was kept at 50±2%. In order to obtain consistant lengths, all the amalgam mix was introduced to the die prior to condensation. Care was taken to minimize shock loading of the plunger by the load. The weight was eased onto the plunger. Gloves were worn during the specimen preparation to minimize moisture contamination of the specimen and dies. If the schedule listed in Table 2 was not followed accurately, the sample was discarded. The dies were cleaned, following each specimen preparation, with acetoneand cotton swabs.

(a) Trituration

(b) Removal of Amalgam from Capsule

(c) Introduction of Amalgam to Die

(d) Application of Pressure

(e) Removal of No. 2 Spacer

(f) Ejection of Specimen

Figure 6. Preparation of ADA Specimen

Testing Equipment and Procedures

Diametral Compression Test

It was stated earlier that dental amalgam is a brittle material, and the diametral compression test is commonly used to investigate brittle materials. The test is performed by placing a cylindrical

specimen on its side between two platens which exert compressive forces upon the specimen. The sequence of the test involve measuring the diameter and length of the amalgam specimen with a micrometer, wrapping the specimen in a double thickness of aluminum foil and breaking the specimen with a strain rate of 0.02 in/min in the tensile tester.* The specimen is padded with aluminum foil in order to alter the surface stress distributions on the specimens, which result from contact stresses and surface irregularities. Figure 7 illustrates the orientation of the tensile stresses in the specimen.

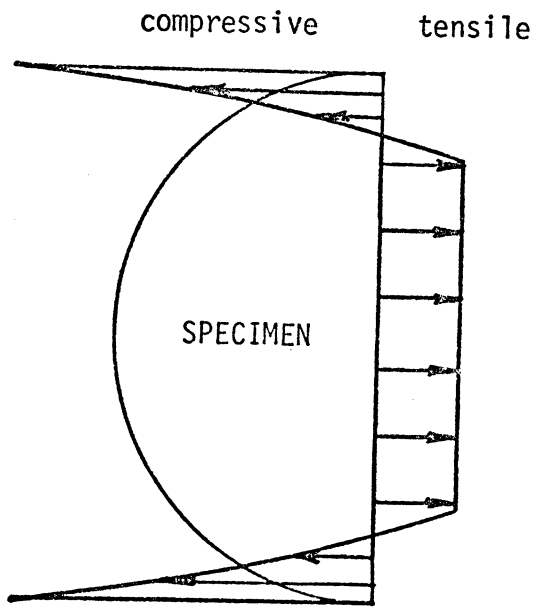

Figure 7. Tensile Stress Distribution in a Diametral Compression Specimen

*Tinius-Olsen Universal Testing Machine, Tinius-Olsen Testing Machine Company, Willow Grove, PA.

The force (P) at fracture, along with the values measured for the length (L) and the diameter (D) of the specimen, are substituted into the following equation to determine the fracture strength (this value is termed splitting tensile strength - STS).

$$STS = \frac{2P}{\pi DL}$$

A controversy has arisen regarding the validity of the value obtained from the previous equation. In fact, the STS value seems to be approximately 60% of the fracture strength as determined by a uniaxial tensile test for the same material. The Theory of Elasticity derivation of the prior equation requires the satisfaction of certain assumptions; the above strength discrepancy results when these assumptions are not satisfied experimentally by the diametral compression test on amalgam (see Lewis (1972) for the details of this controversy).

Static Creep Test

A clinical study (Terkla and Mahler, 1964) revealed the phenomenon of marginal extrusion of some amalgam restorations; presumedly this is a manifestation of flow. Although the clinical significance of extrusion is not yet a matter of consensus, it is reasonable to assume that this phenomenon represents a condition deleterious to the quality of the restoration.

Mahler and Van Eysden (1969) have modified existing engineering creep study techniques to evaluate the time-dependent deformation of dental amalgam. A 5250 psi static compressive load is applied to a 4mm (diameter) X 8mm amalgam cylinder maintained at 98.6±1°F for a four hour time duration. The change in length of the specimen is monitored by a differential transformer, and the output of this transformer is recorded and interpreted to produce a deformation versus time plot.

A four-station creep machine was designed and constructed for use in this laboratory. A dead weight loading system was used; it was calibrated with an electronic force transducer to maintain a constant pressure of 5250 psi upon the 4mm diameter amalgam specimen. Mahler and Van Eysden (1969) monitored the creep deformation for a period of four hours following the load application. A description of the creep testing machine used in this investigation is given in Appendix A. Figures 8 and 9 illustrate the creep testing machine and associated electronic recording equipment.

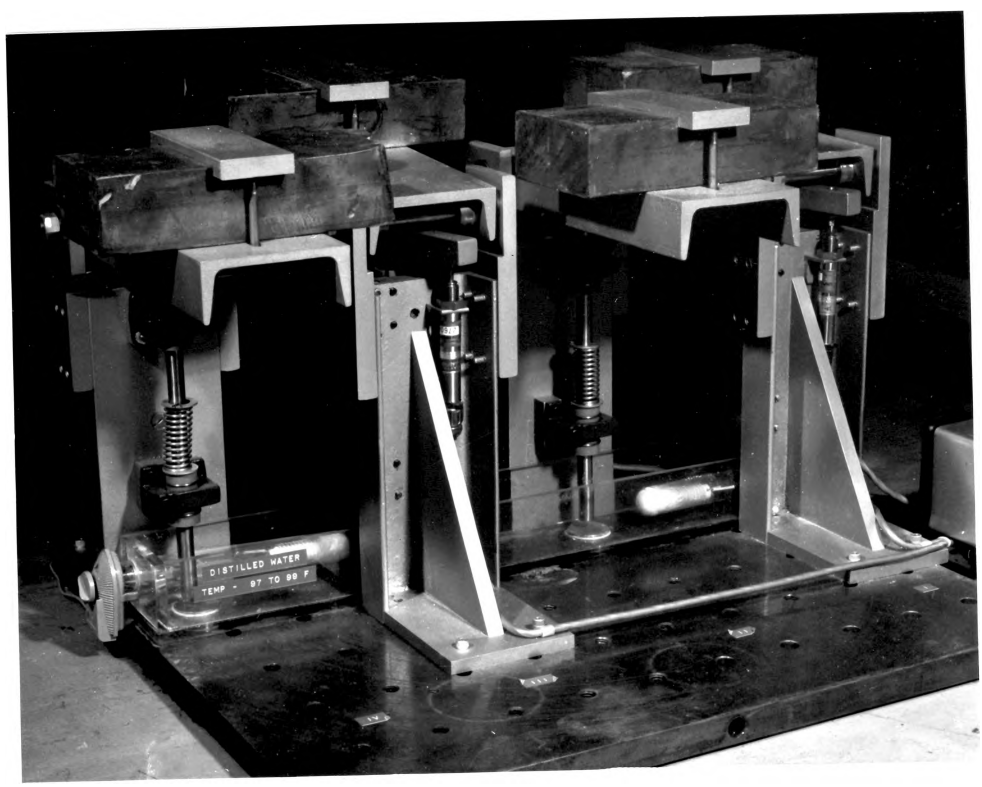

Figure 8. Static Creep Testing Machine

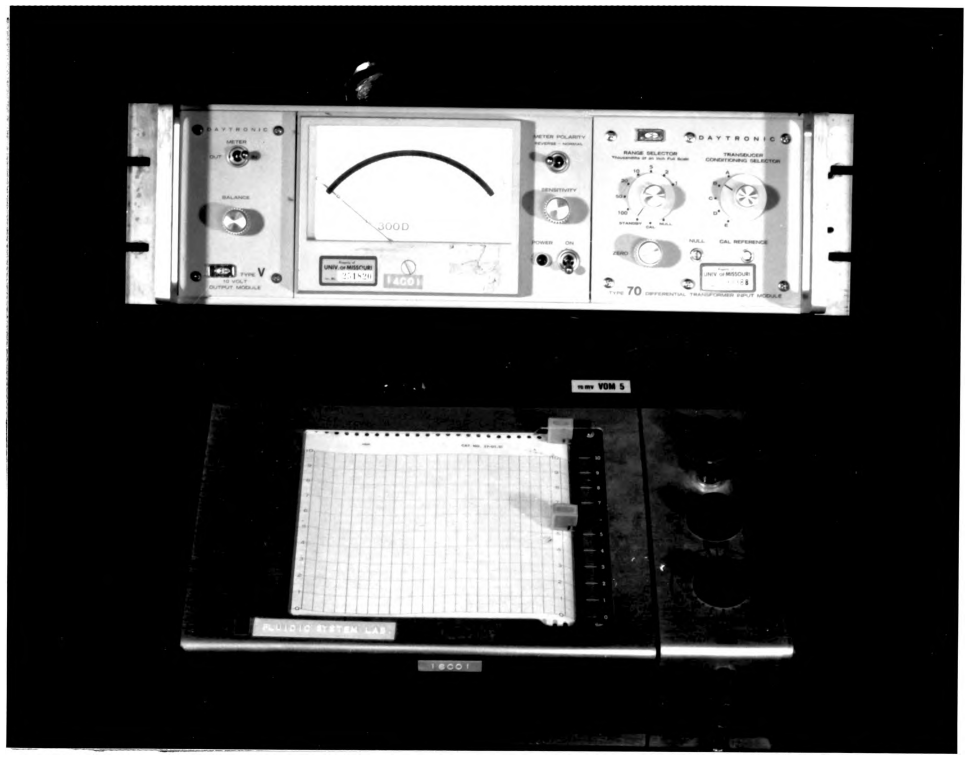

Figure 9. Deformation Recording Equipment

The creep testing procedure involved shortening a standard ADA specimen to 8 mm by grinding in a standard machine shop platform grinder. Care was taken to not overheat the specimen. The ground specimen was placed in the constant temperature water bath and was allowed to assume the temperature of the bath prior to the test. The differential transformer and recorder were then zeroed so that the recorder showed no deformation when the test began. The 5250 psi compressive load was applied, and the deformation was monitored for four hours. A typical creep curve is displayed in Figure 10.

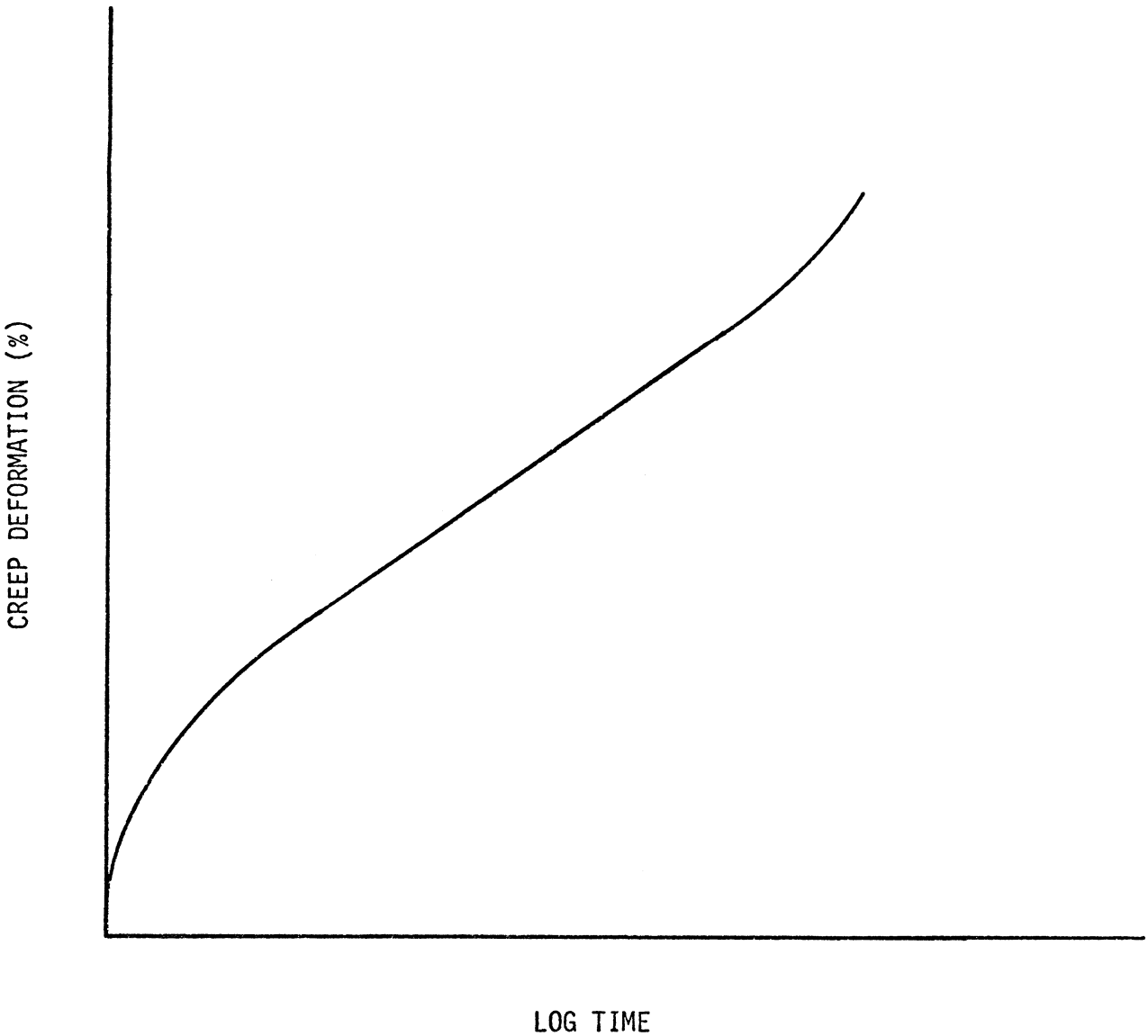

Figure 10. Typical Creep Curve for Amalgam

It was later observed that the elastic strain observed for Dispersalloy specimens is exceedingly small when compared to the plastic creep strain, both being measured for a load of 5250 psi. Therefore, to simplify the test only the initial and final lengths of the specimen were measured with a micrometer. The electronic equipment was used only to monitor the similarity in shapes of the creep curves; no detectable differences were observed in the shapes of the curves.

Microstructure Preparation

Mounting and Polishing

No special techniques or equipment are necessary for the metallographic polishing of dental amalgam. However, the polishing time and pressure required to obtain a satisfactory microstructure are both considerably less than for most engineering materials. Extreme care must be exercised during polishing; therefore, hand polishing on a mechanical wheel yields more satisfactory results than when complete automation of polishing is used.

The standard ADA specimens were used for the microstructural investigations; they were mounted in cold mounts due to the relatively low melting point of the amalgam. Clear-cast*, a product available at hobby stores, was allowed to harden about the amalgam specimen; the specimen had been placed within a one inch I.D. brass ring. The resin was allowed to harden overnight.

Rough polishing was performed on 600 grit emery paper** with a water coolant. Light hand pressure was maintained until a bright, new surface covered the entire cross-section of the specimen. The specimen was then washed in running water, followed by a water wash in an ultrasonic cleaner for two minutes. The specimen was removed from the ultrasonic cleaner and dried with a compressed air blast.

Fine polishing was performed on successively finer grit diamond paste*** on microcloth+. An oil base coolant was used during this

---

* Clear cast, American Handicrafts Company, Forth Worth, Texas.
** Emery Paper, Buehler Ltd., Evanston, Illinois.
*** Metadi Diamond Paste, Buehler Ltd., Evanston, Illinois.
+ Microcloth, Buehler Ltd., Evanston, Illinois.

procedure. The specimen was washed following each polishing step according to the following sequence: running water wash, warm soapy water ultrasonic wash, followed by air blast drying. Successive diamond paste grit sizes of 9μ, 6μ, 1μ and 1/4μ were used in the polishing procedure. Polishing at each step continued until the scratches from the prior step were removed.

Dental amalgam, like some engineering materials, consists of different phases with radically varying hardnesses. As a result, when polishing is prolonged, the material experiences relief polishing. Hard particles are pulled from the microstructure and are ground across softer areas by the polishing wheel. Uncontrolled scratching occurs across the microstructure. To minimize this problem, reduced polishing pressure and time were used.

Etching

Certain experiments in this investigation required an etched microstructure. Many etching reagents have been identified for use on amalgam microstructures. For this study, a mild etchant was required to remove a surface smear which resulted from fine polishing.

An etch comprised of two parts hydrogen peroxide (3%), five parts ammonium hydroxide (30%) and five parts water proved to be the most satisfactory. This etchant was used to remove the surface smear. The etchant, however, proved to be unsatisfactory for microprobe analysis since it also leached copper from some phases in the microstructure.

CHAPTER III

EXPERIMENTAL RESULTS

Mechanical Testing

As stated in the introduction, the evaluation of the time-dependent variation in the mechanical properties of Dispersalloy was an initial objective of this investigation.

Six groups, consisting of twenty-five standard ADA specimens each, were prepared as prescribed by the specifications stated in the previous chapter. Each group of amalgam specimens was allowed to age for different times prior to mechanical testing.

Reports generally agree that the setting strength of conventional dental amalgam is well developed in 24 hours (Pires, et al., 1969). Following the 24 hour period, the remaining strength increase is normally complete by the end of the first month after specimen preparation. Hence, the groups were allowed to age according to the following schedule so that the one month period could be adequately described: one day, four days, one week, two weeks, three weeks and one month.

Each group of twenty-five specimens was divided so that twenty specimens were subjected to the diametral compression test, four specimens were submitted to the creep test, and the remaining specimen was retained as a spare in case any difficulties arose in the testing of the other specimens.

The diametral compression test results obtained from the six Dispersalloy specimen groups are tabulated in Table 3. The mean and standard deviation of the individual strength values are indicated in the table.

TABLE 3

Time-Dependent Tensile Strength of Dispersalloy Amalgam

Age (days)	Tensile Strength (psi)
1	7467±978
4	7246±578
7	7298±816
14	7656±647
21	7786±596
28	7437±857

No definitive conclusions can be made from the strengths due to the large standard deviations inherent in the data. The test data are useful when large strength variations are expected; however, no significant strength changes occurred during the one month ageing period.

Apparently, the microstructural changes occurring during this period do not significantly alter the tensile properties of the Dispersalloy amalgam. In this respect, Dispersalloy behaves quite similarly to conventional amalgams. Furthermore, the microstructural changes which occur during the first day following preparation must be predominately responsible for the tensile strength characteristics displayed by Dispersalloy.

Unlike the tensile test, the creep studies performed on the same six age groups yielded results which indicate that the creep rate reduction is directly related to the increased age of the Dispersalloy amalgam. Four standard ADA specimens from each age group were investigated by the static creep test described in Chapter II. Both Table 4 and Figure 11 indicate the results obtained from the time-dependent creep study. The static creep tabulated for each group is the mean calculated from four test results. These results are determined by the following equation, where ΔL is the four hour creep deformation and L_o is the original length of the undeformed specimen.

$$\text{STATIC CREEP (\%)} = \frac{\Delta L}{L_o} \times 100\%$$

TABLE 4

Time-Dependent Static Creep of Dispersalloy Amalgam

Age (days)	Static Creep (%)
1	0.9523
4	0.7619
7	0.6984
14	0.6032
21	0.5714
28	0.5397

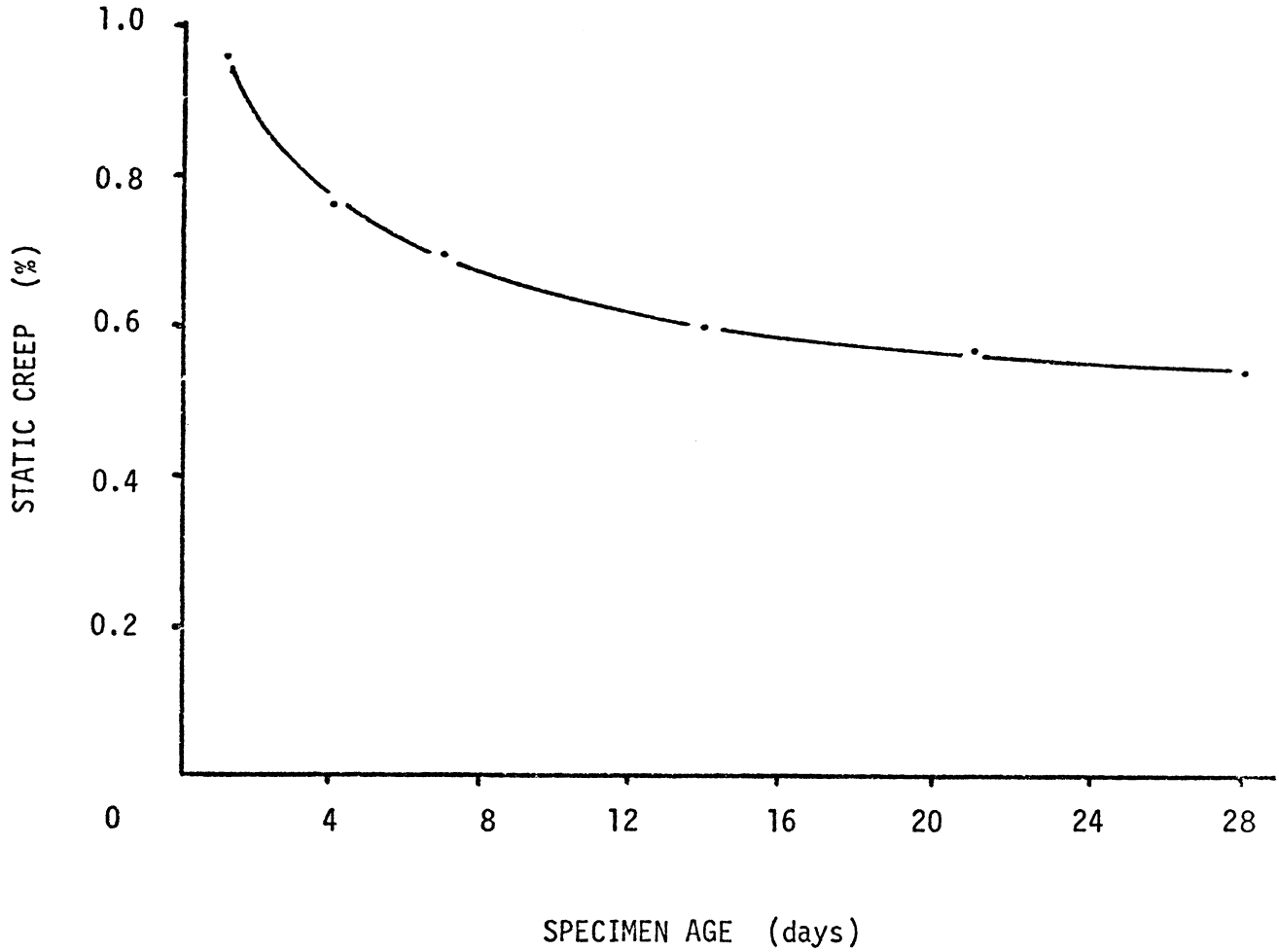

Figure 11. Static Creep Test of Aged Dispersalloy

Since a continued decrease in creep rate was observed with increasing specimen age, some microstructural changes must be occurring during the month following specimen preparation. This conclusion was not indicated as a result of the diametral compression test. It can be concluded therefore, that different microstructural phenomena must govern the two mechanical properties being considered.

The importance of grain boundaries in defining the tensile strength characteristics of dental amalgam was discussed in the introduction of this report. As stated earlier, no significant variation in tensile strength was observed during the first month following specimen prepar-

paration. Since the grain boundaries are formed immediately following trituration of the amalgam components, the microstructural changes which occur during this first month apparently do not alter the grain boundary cohesion within the amalgam.

In order to evaluate the hypothesis that the creep of amalgam is predominately a result of deformation within the matrix grains, an experiment was designed to metallographically examine scratches left on specimens prepared from Dispersalloy and a fine-cut amalgam. The two specimens were prepared according to the ADA specifications, which produce 4mm (dia.) cylinders 8 mm in length. A flat surface was ground along the side of each cylinder. These flat surfaces were metallographically polished to a 1/4 micron smoothness in a manner similar to that described earlier. However, the specimens were not mounted. Care was taken to see that scratches remained in the polished microstructure following metallographic preparation. Each polished specimen was subjected to the four hour creep test like that described in Chapter II. Figures 12 and 13 are photomicrographs (160X) of the Dispersalloy and fine-cut amalgams following the creep test. The scratches remained continuous across the grain boundaries in both figures indicating that neither grain boundary migration nor grain boundary sliding occurred. By placing a straight-edge along the scratches, it can be observed that some rotation of the grains has occurred. This rotation is indicative of plastic deformation within the grain. The polishing scratches in the fine-cut amalgam (Fig. 13) were observed to rotate approximately 2.5° when measured across an Ag_3Sn particle. A similar measurement on polishing scratches in the Dispersalloy microstructure (Fig. 12) yielded a one degree rotation.

Figure 12. Dispersalloy Creep Specimen Photomicrographs (160X)

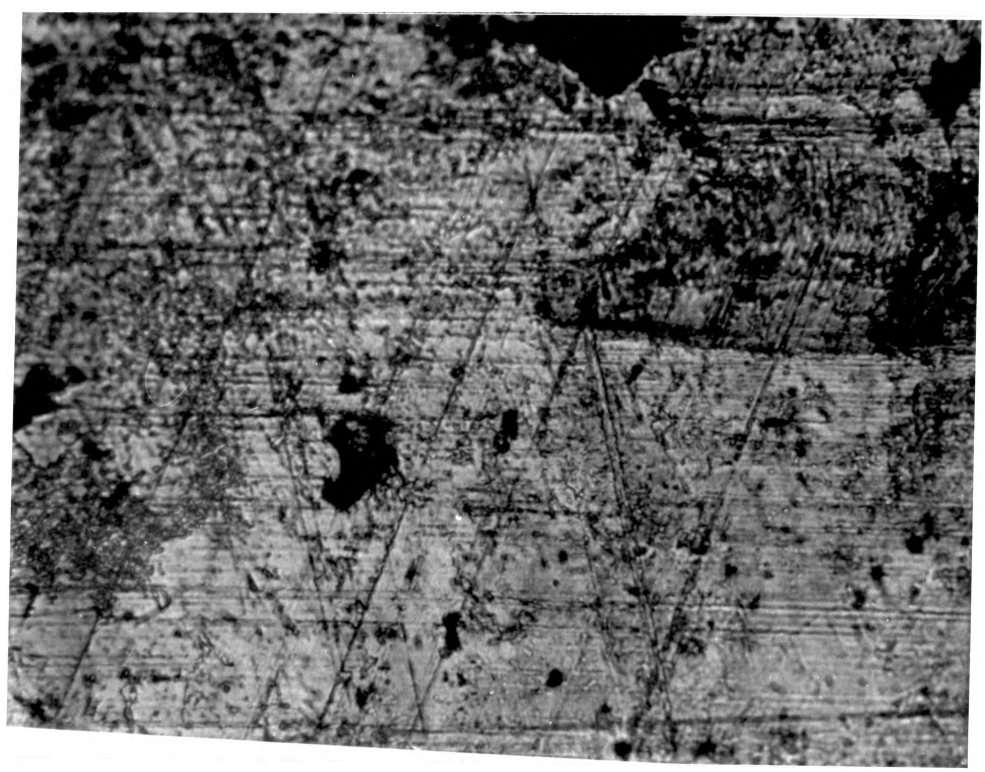

Figure 13. Fine Cut Amalgam Creep Specimen Photomicrograph (160X)

The fine-cut amalgam microstructure experienced more grain rotation than did the Dispersalloy microstructure, and the total creep deformation of the fine-cut amalgam was nearly twice that of the Dispersalloy specimen. The absence of grain boundary sliding requires that the creep deformation be solely accommodated by the intragranular deformation. Dispersion hardening cannot explain this observation; rather, some other hardening mechanism must be involved.

Microstructure Study

As an aid in identifying the hardening mechanism responsible for the improved amalgam creep characteristics and to characterize the microstructure of Dispersalloy, electron microprobe analysis was performed on a polished Dispersalloy specimen. The electron microprobe analyzer is an instrument capable of accurately measuring the surface chemical composition of amalgam specimens. Analysis is accomplished by measuring the intensity and wavelength of characteristic x-rays generated below the specimen surface by an incident electron beam. The electron beam is focused upon the specimen surface. The micron diameter beam allows the chemical analysis of microscopic sample areas. A more complete discussion of the investigative capabilities of the electron microprobe analyzer is presented in Appendix B.

A standard ADA Dispersalloy specimen was metallographically mounted and polished according to the procedures presented in Chapter II. A one day old Dispersalloy specimen was used for the initial electron microprobe study. In this initial study, x-ray area scans were generated in order to identify the locations (phases) containing concentrations of the four major constituents: silver, tin, copper and

mercury. Figure 19 displays results similar to those determined in the first microprobe study. Light areas in the photographs represent areas containing concentrations of the specific element being analyzed. It was immediately apparent that the copper-silver spheres act as sinks for the tin that is released when mercury reacts with the Ag_3Sn alloy particles to form the Ag_2Hg_3 matrix phase. In conventional amalgam systems, the released tin reacts with mercury to form the gamma-2 (Sn_{7-8} Hg) phase. However, in Dispersalloy the tin preferentially replaces silver in the copper-silver spheres before the gamma-2 phase can form. This occurrence has been termed the formation of the tin ring. Only isolated formation of the gamma-2 platelets has been observed. The formation of the tin ring is largely responsible for the corrosion resistance behavior of Dispersalloy restorations. As stated in the introduction, the degradation of the gamma-2 phase is largely responsible for the poor corrosion resistance of conventional amalgams.

In addition to observing the tin ring about the copper-silver eutectic spheres, a series of particles were detected along the interface between the sphere and the ring. X-ray area scans indicated that these "emissary" particles were merely a result of polishing or were in fact a part of the Dispersalloy microstructure.

Johnson (1972) claims that these particles are mercury-rich corrosion products. He further states that this observation is compatible with the theories of Jorgenson (1965) with regard to the mechanism of amalgam corrosion. Mahler et al. (1973), on the other hand, claim that these same particles have a concentration similar to the γ_1 (Ag_2 Hg_3) phase, and therefore they are probably a result of mass

transfer during polishing. Further analyses of this problem were performed in this laboratory, and the results will be provided in a later section of this chapter.

Several weeks passed before the electron microprobe analysis could be resumed. The same specimen was used for the study and had correspondingly aged several weeks. When additional Ag, Sn, Cu and Hg x-ray area scans were produced, it was observed that the thicknesses of the tin rings were increasing, and the size and distribution of the emissary particles were changing. The particles were increasing in size and were seemingly migrating to the center of the spheres.

The changing microstructure became suspect in explaining the varying mechanical properties of the Dispersalloy amalgam. It was therefore concluded that a microprobe investigation should be conducted of specimens corresponding to the six ages used in the mechanical properties study: one day, four days, one week, two weeks, three weeks and one month. Figures 19 through 24 in a later section of this chapter were produced in this ageing investigation.

To conclude the initial microprobe study, intensity point counts were produced for each phase in order to determine the average compositions of each microstructural phase. This standard microprobe procedure is described in Appendix B. Of significance was the presence of 3-5 weight percent copper within the unreacted Ag_3Sn particles and the Ag_2 Hg_3 matrix. This concentration of copper was not expected to be present in either the γ_1 or γ phases from a consideration of the manufacturer's published alloy specifications. It must be recognized that the presence of only a few percent of a solute alloying element in a differing solvent material is sufficient for considerable solution

hardening of the matrix grains certainly compliments the experimental results gained from the prior mechanical testing. Additional experimentation was planned to determine the source of the copper solute atoms and the distribution of copper in the γ_1 matrix phase.

At this time, a brief discussion of the Dispersalloy microstructure will be presented so that the metallurgical problems stated earlier in this section can be more easily understood by the reader. The four-color micrographs shown in Figures 14a and 14b and Figures 15a and 15b are x-ray area scans produced on an electron microprobe.* Each micrograph is a two-color composite containing two x-ray area scans in one photograph. Figures 14a and 15a were produced with copper Kα radiation displayed through a red filter, and with mercury M radiation displayed through a green filter. In like manner, Figures 14b and 15b were produced with tin Lα radiation displayed through a yellow filter, and with silver Lα radiation displayed through a blue filter. The area under analysis on the Dispersalloy specimen was 50μm square.

The black areas in Figure 14a and 15a and the white areas in Figures 14b and 15b represent the unreacted Ag_3Sn particles often called the gamma phase. The red areas in Figures 14a and 15a and the blue areas in Figures 14b and 15b indicate the copper-silver spheres. Yellow areas in Figures 14b and 15b show high concentrations of tin; notice should be taken of the tin rings surrounding the copper-silver eutectic spheres. The emissary particles appear as yellowish spots on the red background in Figures 14a and 15a. Also of interest is the white interface "ribbon" separating the copper-silver sphere and the tin ring in

* Model EMX, Applied Research Laboratories, Sunland, California.

Figures 14b and 15b. This white ribbon is an indication that the interface composition is similar to the Ag_3Sn particles. The green area in Figures 14a and 15a and the black area in Figures 14b and 15b are the γ_1 (Ag_2 Hg_3) matrix phase.

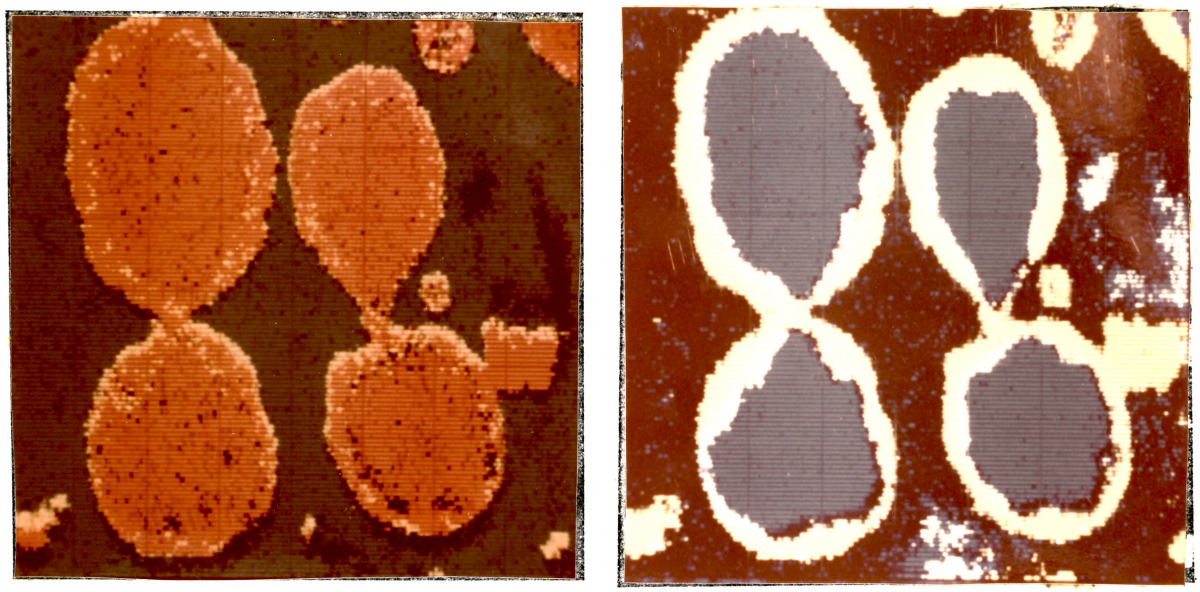

a b

Figure 14. Four-Color X-Ray Micrograph of Dispersalloy

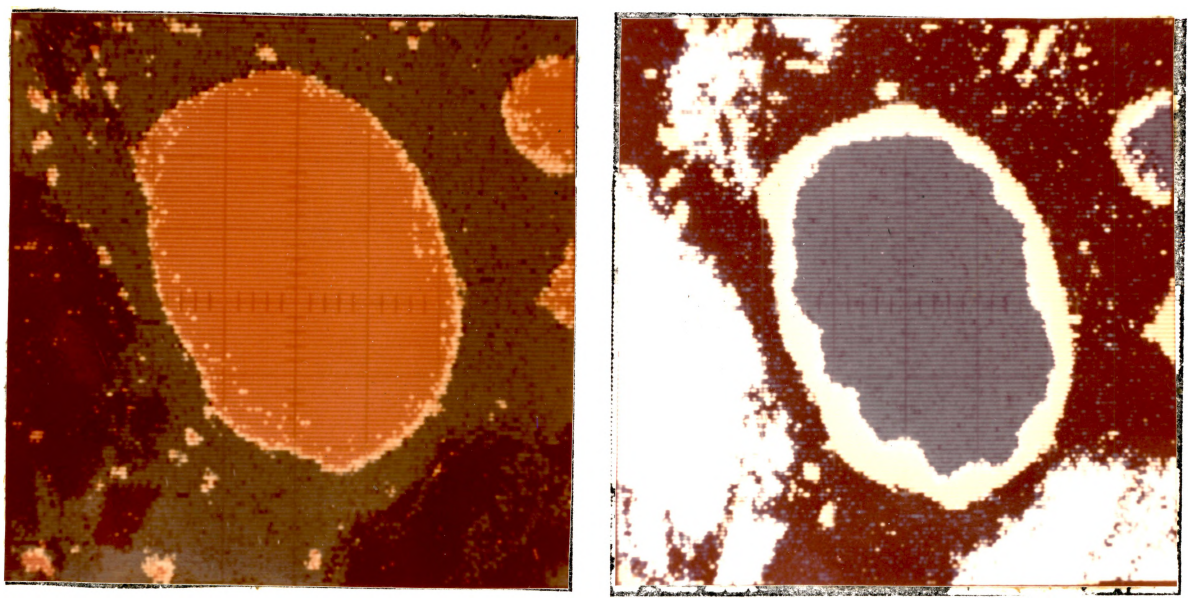

a b

Figure 15. Four-Color X-Ray Micrographs of Dispersalloy

Emissary Particle Study

The emissary particle controversy concerns whether their origin is a natural corrosion process (Johnson, 1972) or is a polishing contamination problem (Mahler , et al., 1973). It had already been observed by this researcher that a surface smear resulted during metallographic polishing of Dispersalloy. This smear could be observed in an optical microscope. The etchant described in Chapter II was used to remove the smear layer from the microstructure; the emissary particles were also removed in this process. The surface adhesion between the particles and the microstructure was therefore no greater than was the polishing smear coating. However, no insight into the origin was gained from this exercise.

A freshly prepared ADA Dispersalloy specimen was fractured by shock loading (shock loading of amalgam often leads to intragranular fracture). The objective was to obtain a fracture surface through a copper-silver sphere so that the presence or absence of emissary particles there could be determined. The fracture surface was viewed in a scanning electron microscope; the discussion of the theory and use of this instrument is contained in Appendix B. Only a few of the copper-silver spheres were fractured; however, no emissary particles were observed.

At this time, the availability of an ion microprobe analyzer* became known. This instrument is capable of chemical analysis of surfaces in a manner analogous to the electron microprobe analyzer. However, the instrument utilizes a focused ion beam rather than an electron beam. The highly energized ion beam causes material to be sputtered, in the

---

* Applied Research Laboratories, Sunland, California.

form of ions, from the specimen surface. The sputtered ions are analyzed in a mass spectrometer in order to identify the composition of the specimen. The ion beam erodes the surface of the specimen, and analysis can be afforded at varying desired depths. A more complete description of the operation of this instrument is contained in Appendix B. The usefulness of this instrument can be appreciated when the presence of a contamination layer has formed on the specimen surface. The ion microprobe has the capability to burrow through this layer, to penetrate to the true microstructure. Area scans were produced for the four major constituents: silver, tin, copper, and mercury. The surface was eroded for a period of time by the ion beam, and then a series of area scan micrographs were produced. This procedure was repeated several times so that analysis could be completed at various depths within the copper-silver spheres. No emissary particles were observed at any depth. Figure 16-a,b,c,d illustrate one set of area scans obtained in this study.

One further experiment was designed to answer the emissary particle controversy. A freshly polished Dispersalloy ADA specimen was viewed at 2000 X magnification in a scanning electron microscope.

The emissary particles were immediately observed on all silver containing phases, Figure 17. Upon further investigation, several emissary particles were detected as overlying polishing scratches, Figure 18. The presence of particles inside the scratches indicates that the formation of the particles was a result of the polishing sequence. Hence, Mahler (1973) was correct when he stated that the particles were merely polishing artifacts.

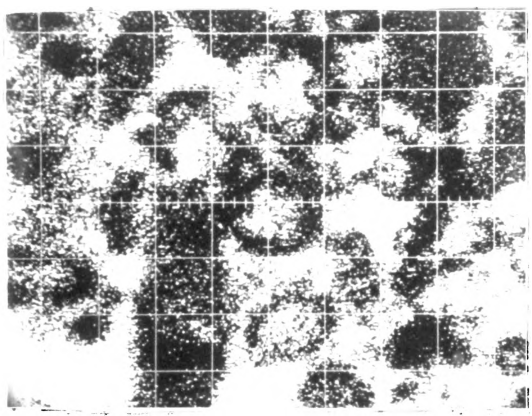

a. Silver

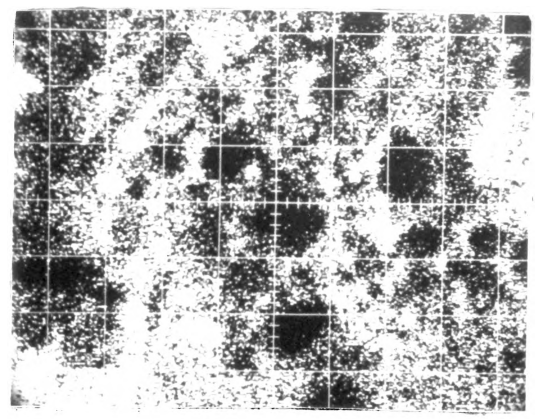

b. Tin

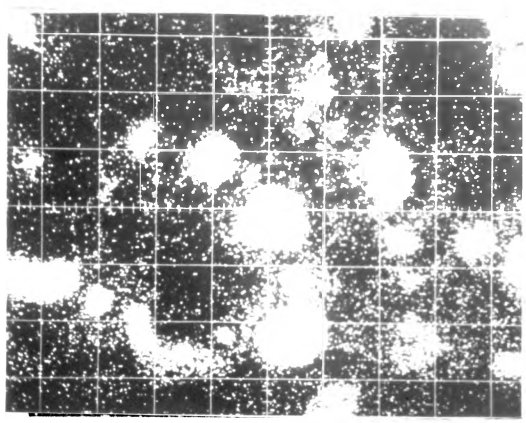

c. Copper

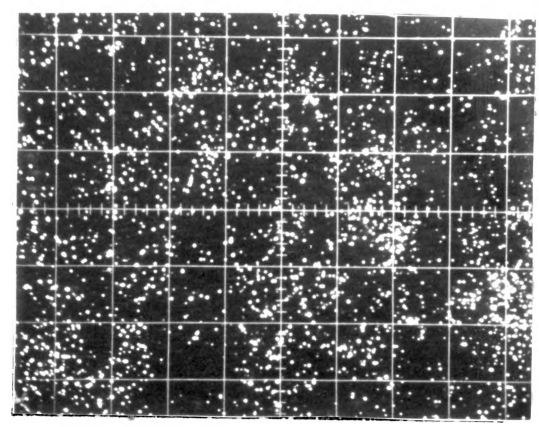

d. Mercury

Figure 16. Ion Microprobe Area Scans of Dispersalloy

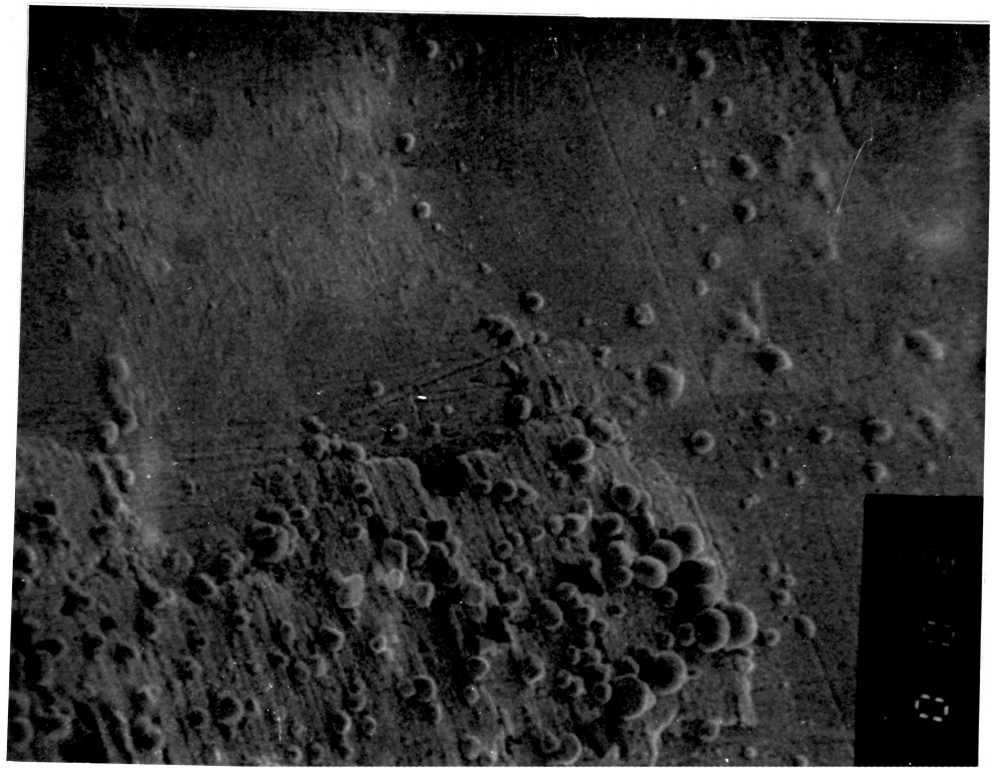

Figure 17. Scanning Electron Micrograph of Polished Dispersalloy

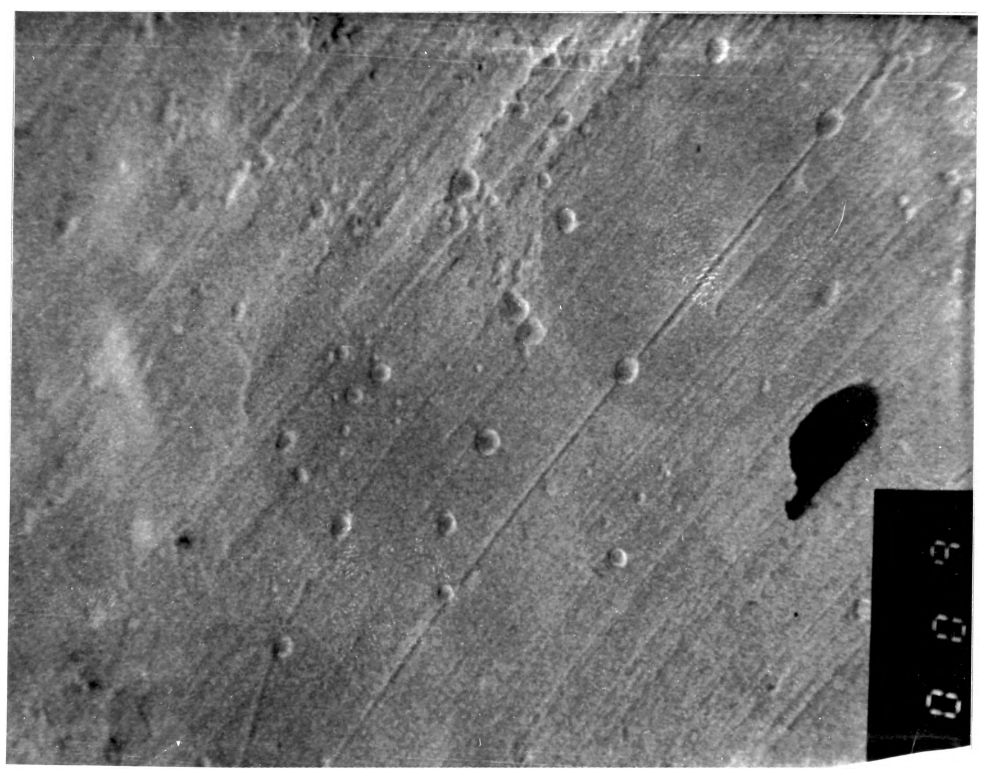

Figure 18. Emissary Particles Within Polishing Scratches in Dispersalloy

Hardening Mechanism

When the presence of 3-5 weight percent of copper was located in the Ag_3Sn particles and in the $Ag_2 Hg_3$ matrix the likelihood of solution hardening was interpreted as a challenge to the manufacturer's claims of dispersion hardening. Mechanical testing had made the possibility of dispersion hardening improbable. The source of the solution strengthening needed to be considered. Two possible sources of copper solute atoms are present in the unmixed amalgam components: the alloy powder and the mercury. The alloy powder contains Ag_3Sn particles known to contain 3-5 weight percent copper and copper-silver eutectic spheres. It was believed that the copper in the eutectic spheres would combine with tin in the tin ring and therefore not be a source of copper solute atoms.

The copper-mercury phase diagram (Constitution of Binary Alloys, 2nd Ed., 1958) indicates that the maximum solubility of copper in mercury at room temperature is 32 ppm. However, if the mercury and copper were combined with another element in some ternary compound a much greater concentration of copper could be expected. Atomic absorption analysis was performed on mercury contained in a fresh Dispersalloy capsule. It was determined that, at room temperature, the mercury contains the maximum solubility of copper, 32 ppm. This amount of copper is insufficient to solute harden the γ_1 matrix.

Electron microprobe analysis was performed on the Dispersalloy alloy powder. It was desired to determine if copper was present in the Ag_3Sn particles prior to trituration in sufficient quantities to explain the 3-5 weight percent concentration in the $Ag_2 Hg_3$ matrix. The alloy powder was mounted in the cold mount used for the ADA standard specimens.

The surface containing the embedded powder was stroked against the 600 grit emery paper described in Chapter II. The purpose of this simple grinding procedure was to expose the interior of the Ag_3Sn particles for microprobe analysis. Electron microprobe analysis performed on the Ag_3Sn particles indicated that 3-5 weight percent copper was uniformly distributed within Ag_3Sn particles.

Confirmation of the copper solution hardening of Dispersalloy was gained in a conversation with one of the amalgam's developers (Moser, 1974).

Time-Dependent Microstructure Study

The importance of a time-dependent microstructure investigation was emphasized by both the variation in creep resistance and the increase in the tin ring thickness as a function of specimen age. Three differing types of electron microprobe analysis were performed on Dispersalloy specimens with ages corresponding to the six age groups used for the mechanical testing.

Secondary electron images and characteristic x-ray area scans were produced for a visual display of the microstructure phase concentrations. X-ray intensity counts were measured for each of the primary microstructural areas to determine the phase concentrations quantitatively. Finally, matrix line scans* were performed on specimens from the six age groups in order to acquire the diffusion characteristics of various constituent atoms through the Dispersalloy microstructures.

Figures 19 through 24 represent the micrographs prepared from secondary electron images and x-ray area scans. Preliminary observation

* A discussion of this technique is presented in Appendix B.

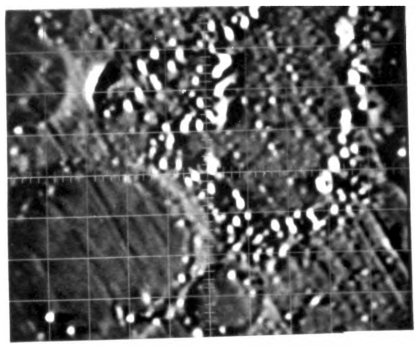

SECONDARY ELECTRONS

ELECTRON MICROPROBE SCANNING IMAGES
DISPERSALLOY DENTAL AMALGAM

AGE: 1 DAY

AREA: 40 x 50 μm

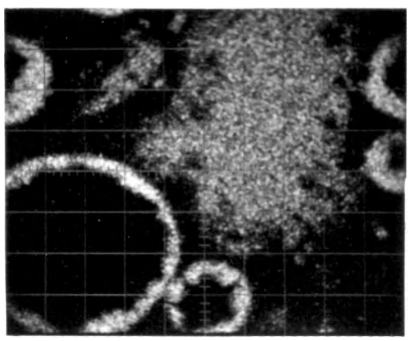

TIN

SILVER

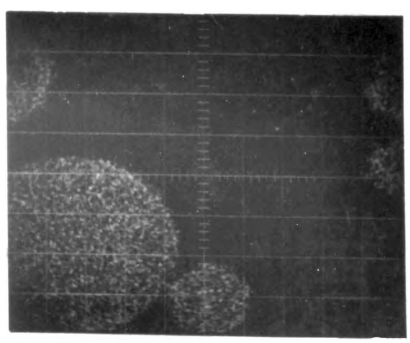

COPPER

MERCURY

Figure 19. X-ray Area Scans of Dispersalloy, Age One Day

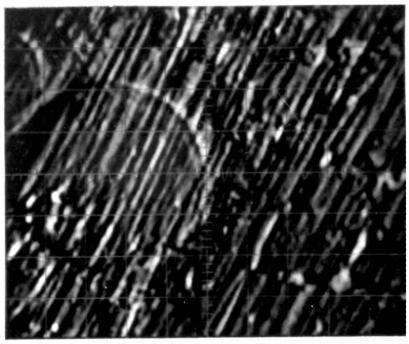

ELECTRON MICROPROBE SCANNING IMAGES
DISPERSALLOY DENTAL AMALGAM

AGE; 4 DAYS

AREA: 40 x 50 μm

SECONDARY ELECTRONS

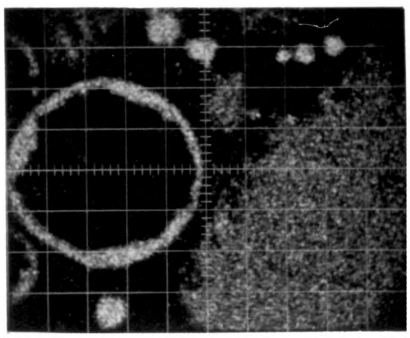

TIN

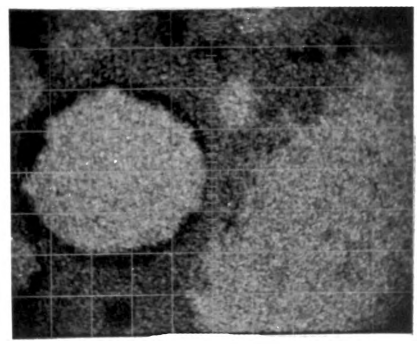

SILVER

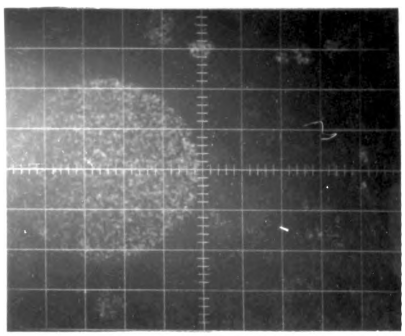

COPPER

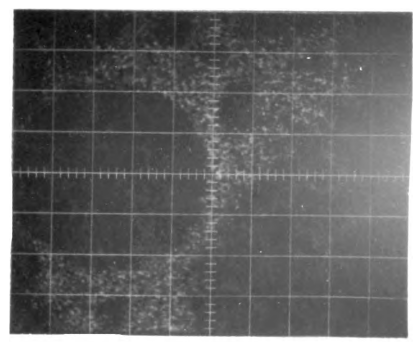

MERCURY

Figure 20. X-ray Area Scans of Dispersalloy, Age Four Days

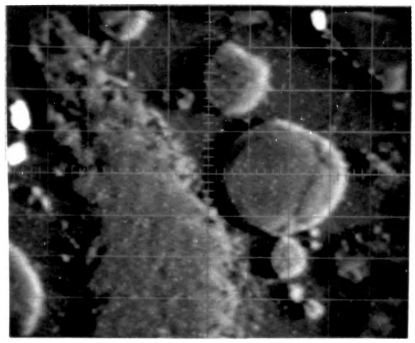

SPECIMEN CURRENT

ELECTRON MICROPROBE SCANNING IMAGES
DISPERSALLOY DENTAL AMALGAM

AGE: 7 DAYS

AREA: 40 x 50 μm

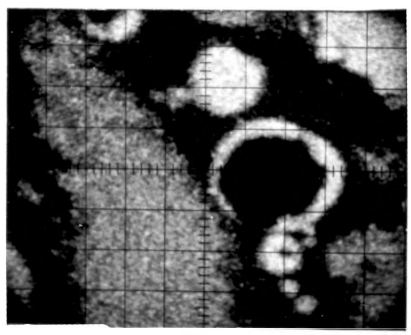

TIN

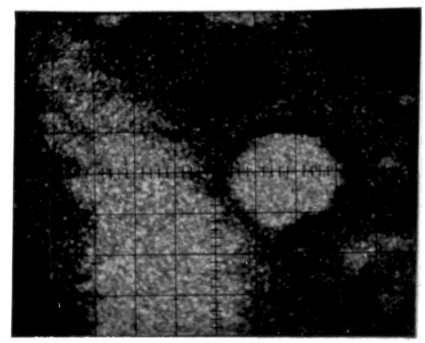

SILVER

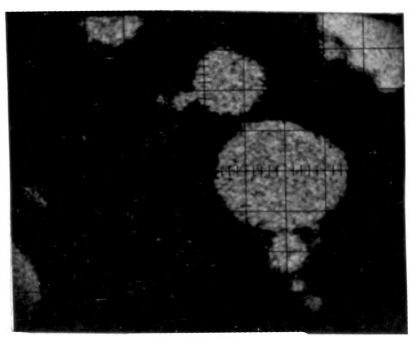

COPPER

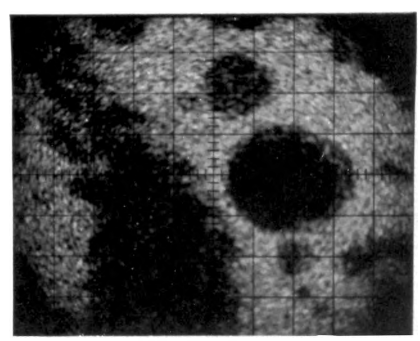

MERCURY

Figure 21. X-ray Area Scans of Dispersalloy, Age One Week

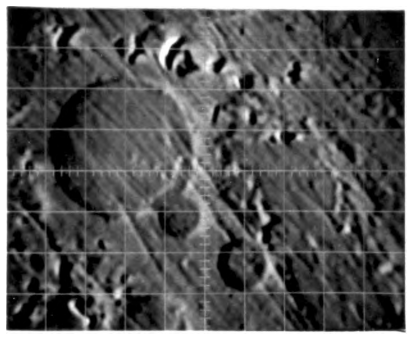

SECONDARY ELECTRONS

ELECTRON MICROPROBE SCANNING IMAGES
DISPERSALLOY DENTAL AMALGAM

AGE: 14 DAYS

AREA: 40 x 50 μm

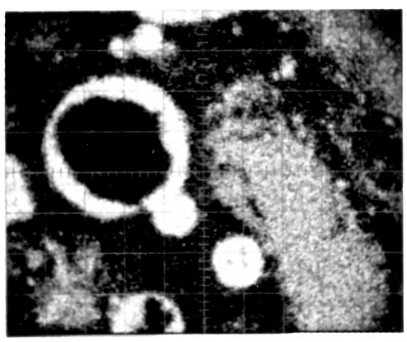

TIN

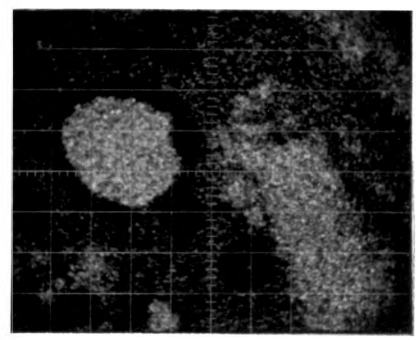

SILVER

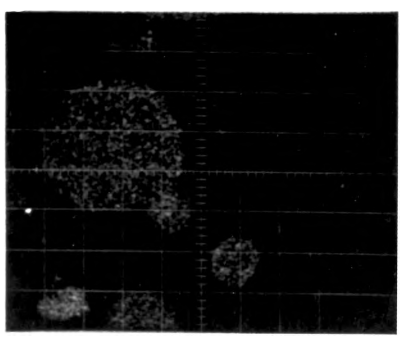

COPPER

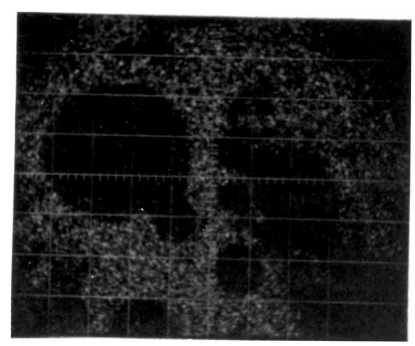

MERCURY

Figure 22. X-ray Area Scans of Dispersalloy, Age Two Weeks

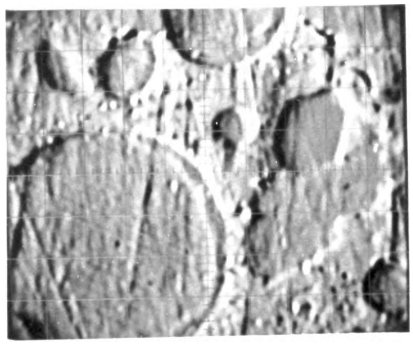

ELECTRON MICROPROBE SCANNING IMAGES
DISPERSALLOY DENTAL AMALGAM

AGE: 21 DAYS

AREA: 40 x 50 μm

SECONDARY ELECTRONS

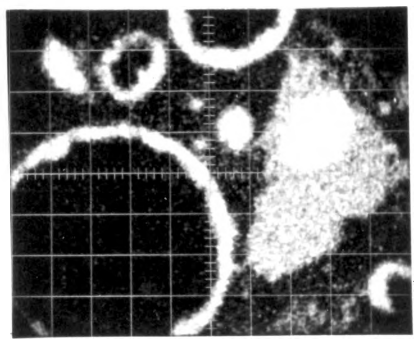

TIN

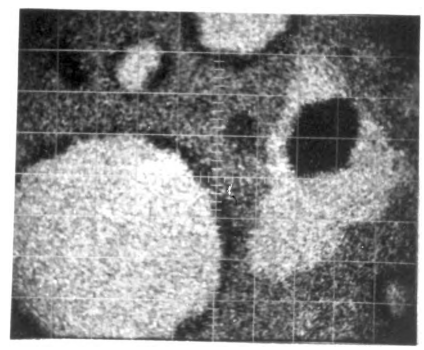

SILVER

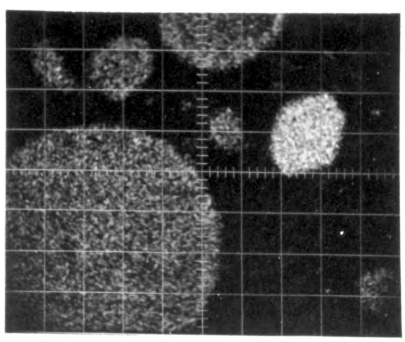

COPPER

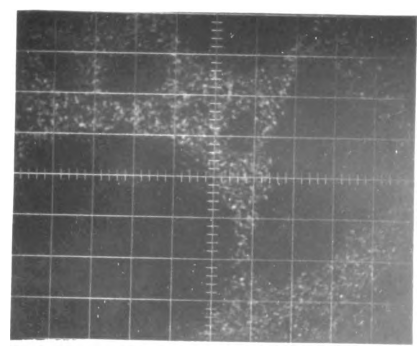

MERCURY

Figure 23. X-ray Area Scans of Dispersalloy, Age Three Weeks

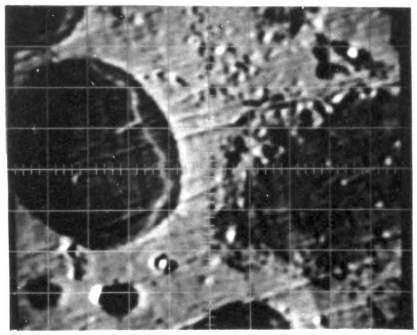

ELECTRON MICROPROBE SCANNING IMAGES
DISPERSALLOY DENTAL AMALGAM

AGE: 28 DAYS

AREA: 40 x 50 μm

SECONDARY ELECTRONS

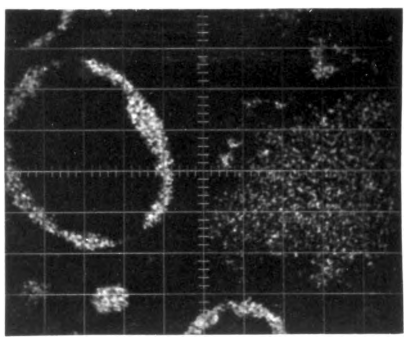

TIN

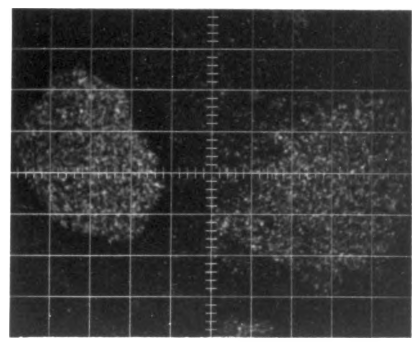

SILVER

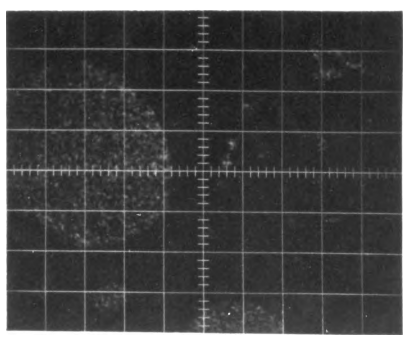

COPPER

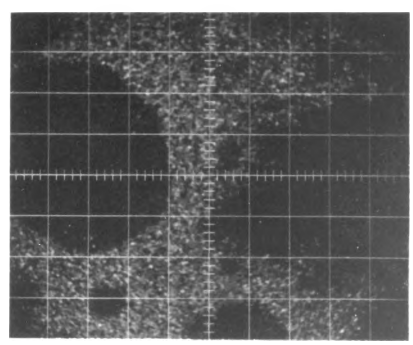

MERCURY

Figure 24. X-ray Area Scans of Dispersalloy, Age One Month

would indicate that the tin rings surrounding the copper-silver spheres do not vary in the expected manner. It must be noted however, the thickness of the tin ring is not only dependent upon specimen age, but the thickness is more dependent upon where the sphere is sectioned during polishing. Therefore, the largest concentration of tin within the ring becomes a more reliable tool for analysis of specimen age. A discussion of this variation in tin concentration will be presented later in this section.

The amount of polishing contamination present upon the specimen surfaces can be observed in the secondary electron images in Figure 19 through 24. The amount of contamination products present varies inversely with the specimen age. This occurrence indicates that hardening of the $Ag_2 Hg_3$ matrix phase increases with age since Mahler et al. (1973) states that the matrix material is the source of the polishing contamination. As the matrix hardens, less contamination product is removed by polishing.

Table 5 indicates the average concentrations in atomic percent of each of the important microstructural areas comprising specimens of the six different ages.

No significant age-dependent concentration variations were measured by this electron microprobe analysis technique as indicated in Table 5. Due to the inhomogeneity of the individual grains comprising the Dispersalloy microstructure, these concentration measurements were location-sensitive. The tabulated concentrations represent average values determined by five separate analyses of each particular phase. An attempt was made to analyze points away from possible concentration gradients resulting from grain boundary effects. A favorable agreement

TABLE 5

PHASE CONCENTRATIONS OF AGED DISPERSALLOY

Microstructural Area Elements Analyzed	CONCENTRATIONS IN ATOMIC PERCENT*					
Copper-Silver Sphere	1 DAY	4 DAYS	1 WEEK	2 WEEKS	3 WEEKS	4 WEEKS
Tin	0.19±0.03	0.30±0.03	0.24±0.04	0.27±0.03	0.21±0.03	0.29±0.03
Silver	60.52±0.39	59.90±0.25	62.50±0.34	59.71±0.46	61.82±0.31	58.82±0.25
Copper	39.07±0.37	39.33±0.23	36.92±0.23	39.81±0.48	37.53±0.31	40.62±0.25
Mercury	0.22±0.11	0.43±0.11	0.35±0.13	0.20±0.09	0.44±0.08	0.27±0.09
Tin Ring						
Tin	35.64±0.16	35.83±0.14	31.92±0.34	35.98±0.20	37.06±0.33	41.35±0.20
Silver	6.38±0.10	8.64±0.32	9.32±0.40	6.37±0.14	5.78±0.19	4.26±0.23
Copper	44.82±0.16	44.10±0.38	48.25±0.29	46.59±0.39	45.54±0.34	47.17±0.33
Mercury	13.13±0.27	11.43±0.25	10.51±0.24	11.05±0.15	11.61±0.32	7.22±0.18
Ag_3Sn Particle						
Tin	24.61±0.18	24.00±0.13	20.36±0.17	23.60±0.09	23.51±0.23	24.22±0.17
Silver	65.69±0.39	71.79±0.14	75.43±0.29	73.91±0.16	70.35±0.12	71.34±0.20
Copper	6.93±0.45	3.11±0.14	1.73±0.14	1.60±0.11	3.03±0.21	1.07±0.13
Mercury	2.77±0.23	1.10±0.07	2.48±0.14	0.89±0.14	3.06±0.16	3.37±0.13
Ag_2Hg_3 Matrix						
Tin	2.93±0.04	2.81±0.05	2.54±0.07	2.31±0.09	3.50±0.10	2.78±0.08
Silver	42.15±0.31	44.53±0.42	43.33±0.28	41.42±0.27	43.09±0.36	44.84±0.29
Copper	0.26±0.09	0.46±0.14	0.42±0.14	0.34±0.06	0.42±0.20	0.32±0.19
Mercury	54.66±0.26	52.20±0.41	53.71±0.31	55.92±0.35	52.99±0.36	52.06±0.19

was obtained in a comparison of these phase concentrations with those of another study (Mahler et al., 1975). Since no concentration variation was identified in the time period ofoone day to one month, the major concentration changes probably occur immediately following trituration, i.e., prior to the twenty-four test.

*Investigators have determined that the phase concentrations, measured by electron microanalysis, are accurate to approximately one percent.

At this point, it should not be concluded that no concentration variability occurs for this is not the case. Only the average concentrations of the particular phases, away from grain boundaries, remain relatively constant. Matrix line scans, mentioned earlier in this section and discussed more completely in Appendix B, were performed on specimens of each of the six age groups to determine the constituent mobility among the microstructural phases.

Horizontal line scans containing eighty points of analysis were performed on the specimens. The resulting data were plotted such that the concentrations of tin, silver and copper were displayed as functions of the position upon the specimen microstructure. The specimens were oriented such that the line scan would traverse the following microstructural areas: Ag_3Sn particle, Ag_2 Hg_3 matrix, tin ring, and copper-silver eutectic sphere. Hence, the migration of constituent elements could be monitored. Of particular interest was the movement of tin from the Ag_3Sn particles to the tin rings surrounding the copper-silver spheres. This technique afforded rapid and accurate investigation of the element concentrations across grain boundaries; it was also helpful in identifying the distribution of copper within the gamma-1 matrix phase. The individual line scan concentration plots are recorded in Appendix D.

Visual analysis of the line scan plots yielded the following results:

(1) A copper-tin phase Cu_3Sn was formed along some of the grain boundaries separating the Ag_3Sn particles and the matrix phase.

(2) The tin concentration of the ring surrounding the copper-silver spheres varied from 34 to 43 weight percent tin. A trend was not observed.

(3) The copper concentration in the $Ag_2 Hg_3$ matrix of the one day specimen varied from 3 weight percent at the Ag_3Sn particle to one weight percent at the tin ring.

(4) A slight copper concentration variation was observed in the four day specimen. No variation was observed in the one, two, three and four week specimens. A seemingly homogeneous distribution of one weight percent copper was measured throughout the $Ag_2 Hg_3$ matrix phase.

(5) High tin and copper mobility was observed in areas between the Ag_3Sn particles and the copper-silver spheres. Apparently, this mobility decreased with specimen age.

(6) High variability of constituent concentrations was observed at all grain boundaries. This is partially due to the very nature of grain boundaries and the amalgam microstructure. Geometric considerations (e.g. surface irregularities) can often times cause variations in measured concentrations.

To summarize the electron microprobe analysis of the aged Dispersalloy specimens, it was observed that no major concentration changes occurred within the amalgam phases, the minor movement of tin and copper within the Dispersalloy specimens proceeded to a uniform distribution of one weight percent copper in the matrix phase and a peak concentration of nearly 43 weight percent tin in the tin ring. Finally the concentration changes at phase interfaces (grain boundaries) seemed to stabilize in the older specimens.

CHAPTER IV

SUMMARY AND CONCLUSIONS

A clinical investigation (Moore and Stewart, 1967) of dental restorations has indicated that 42% of those studied were defective in some manner. Twenty-six percent of all of the restorations examined had fractured in service. A significant portion of dental research undertaken in this century has been devoted to improving the dental amalgam so that the restoration failure rate could be reduced.

Within the last several years, researchers have determined that the propensity for the amalgam margin to creep under masticatory loading extrudes the amalgam material; a poorly supported marginal shelf results from this extrusion. Corrosive attack of the amalgam, in the oral environment, leads to weakening of the marginal shelf by destroying the tin-rich, γ_2 framework. Mercuroscopic expansion, a result of corrosive attack, further extends the amalgam margin. Fracture of the weakened amalgam margin occurs when the local tensile stresses, induced by mastication, exceed the local fracture strength of the amalgam material.

Most recent efforts to improve these three important rheological properties have relied upon modern metallurgical procedures which have been used successfully to improve many engineering materials. A local investigation (Hansen, Holland, Lewis and Moore, 1974) endeavored to alter some mechanical properties of amalgam by eliminating air-borne impurities present during the mixing of the amalgam. Increases in strength of up to 11% were attained by this method, and later analysis indicated that the treated amalgam was also more corrosion resistant.

However, the creep measurement described by Mahler (1969) indicated that the creep rate remained unchanged at a value typical of other fine-cut alloys.

Dispersalloy has been developed within the last twelve years and displays a significant decrease in creep rate and an increased resistance to corrosion. The manufacturer claims that the decreased creep rate results from a dispersion hardening mechanism employed in this radically new amalgam. The product consists of a spherical copper-silver eutectic phase added to a fine-cut amalgam alloy. The ratio of eutectic spheres to fine-cut alloy is approximately 1:2 by weight. Unlike other dispersion hardened alloy systems however, Dispersalloy's tensile strength is somewhat less than many fine-cut amalgams.

Many questions concerning Dispersalloy were unanswered (e.g. the creep hardening mechanism, the explanation for the material's corrosion resistance, and the evaluation of the time-dependent behavior of Dispersalloy). Experiments described in Chapters II and III of this report were designed to gain additional information so that answers to these questions could be formulated.

A comprehensive mechanical testing program was performed on aged Dispersalloy specimens. Test specimens of ages one day, four days, one week, two weeks, three weeks and one month were subjected to the diametral compression test and the static creep test discussed by Mahler (1969).

No significant time-dependent variation in tensile strength was observed in the diametral compression test. The standard deviations of the data are usually large for this test, probably due to void formation within the specimens. However, large strength differences can normally be evaluated by this mechanical test.

Grain boundary cohesion is usually the predominant factor controlling the fracture mode of amalgam; poor grain boundary cohesion results in intergranular fractures (i.e., the crack progresses along grain boundaries). Increased grain boundary cohesion can result in transgranular fracture (i.e., the crack progresses through the grains). The fracture mode, in turn, has a significant effect on the tensile strength of amalgam. Apparently, microstructural changes occurring in the Dispersalloy system do not effectively alter the grain boundary cohesion to such an extent that the alloy's tensile strength is altered.

Unlike the tensile strength, significant hardening was exhibited in the static creep test. Figure 11 in Chapter III illustrates the decrease in creep rate which resulted when older Dispersalloy specimens were examined. As described in Chapter III, metallography has shown that the creep deformation is a result of deformation of the $Ag_2 Hg_3$ matrix phase.

Later microprobe analysis identified the presence of small amounts of copper within the unreacted γ particles and the γ_1 matrix. As the copper solute atoms became more uniformly distributed throughout the γ_1 matrix, Dispersalloy exhibited a decreased creep rate. All mechanical and microstructural testing indicates that the system is solution hardened by the distributed copper concentration within the γ_1 matrix.

Electron microprobe analysis was helpful in understanding other microstructural behavior of Dispersalloy. An initial microprobe study located the presence of tin rings surrounding the copper-silver spheres. During trituration of the amalgam constituents, mercury reacts with both the Ag_3Sn alloy particles and the copper-silver spheres. The silver removed from the spheres during this reaction is replaced by tin liberated during the Ag_3Sn-mercury reaction. This tin combines with copper,

silver and mercury to form the so-called "tin ring". Formation of this ring is beneficial because the tin is then unable to form the deleterious γ_2 phase. It is this phase which is most corrosive and leads to early failure of the amalgam restoration. The absence of the γ_2 framework in Dispersalloy's microstructure no doubt has an effect in lowering the expected tensile strength of the amalgam.

The emissary particles described by Mahler et al. (1973) and Johnson (1972) were determined to be the result of polishing contamination; this determination supports Mahler's hypothesis. The polishing procedure removes mercury-rich material from the Ag_2 Hg_3 matrix and deposits it upon other silver-containing phases (e.g. Ag_3Sn particles and copper-silver spheres). Confirmation of this mechanism was supported by ion microprobe analysis, by fresh fracture surface analysis in the electron microprobe analyzer and by scanning electron microscopy of a freshly polished Dispersalloy microstructure. In the final study, emissary particles were observed within polishing scratches, indicating their presence was not inherent to the specimen metallurgy.

In the time-dependent microprobe study, it was observed that more emissary particle contamination was present in the younger specimens than was present in the older specimens. This mercury-rich contamination was more easily removed from the matrix phase in young specimens because the γ_1 matrix hardens with age. This observation is a further indication that solute hardening is present in Dispersalloy.

Electron microprobe analysis and atomic absorption analysis were performed on the alloy powder and the mercury, respectively. The presence of 3-5 weight percent copper was identified in Ag_3Sn particles

which had been sectioned by polishing and studied in the microprobe. The maximum solubility of copper, in mercury at room temperature, 32 ppm, was measured by atomic absorption analysis. Therefore, only the Ag_3Sn alloy particles contained sufficient concentrations of copper to act as a source for solution hardening. One of the Dispersalloy developers (Moser, 1974) confirmed that the Ag_3Sn particles had been alloyed with small amounts of copper.

Additional microprobe analysis in the time-dependent investigation indicated that the basic phase concentrations do not change as a function of specimen age. Only minor concentration variations were measured when analysis was performed at locations away from other phases.

Matrix line scan analysis showed significant concentration changes of tin and copper within the γ_1 matrix when analysis was performed along a 40μm line connecting an Ag_3Sn particle and a copper-silver sphere. Tin atoms migrate from the alloy particles to the tin rings, and copper diffuses into the γ_1 matrix phase from the Ag_3Sn particles. In the one and four day specimens, high concentrations of both tin and copper were measured at the Ag_3Sn - matrix interface. These concentrations decreased with age. As specimen ageing progressed, the copper solute atoms became more uniformly distributed in the γ_1 matrix phase at a concentration of one weight percent.

In this investigation of Dispersalloy, it was determined that the amalgam's improved creep characteristics are solely a result of copper solute hardening. The material's corrosion resistance results from formation of the tin ring and the general absence of the γ_2 phase.

APPENDIX

APPENDIX A

DESIGN OF CREEP TESTING MACHINE

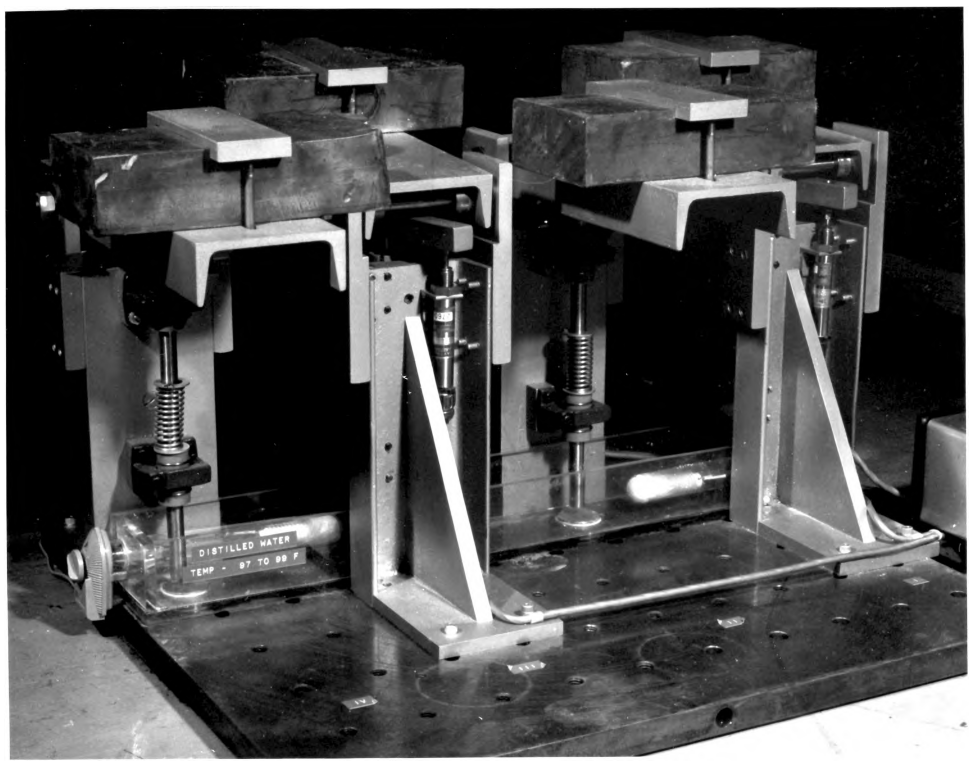

Figure 25. Static Creep Machine

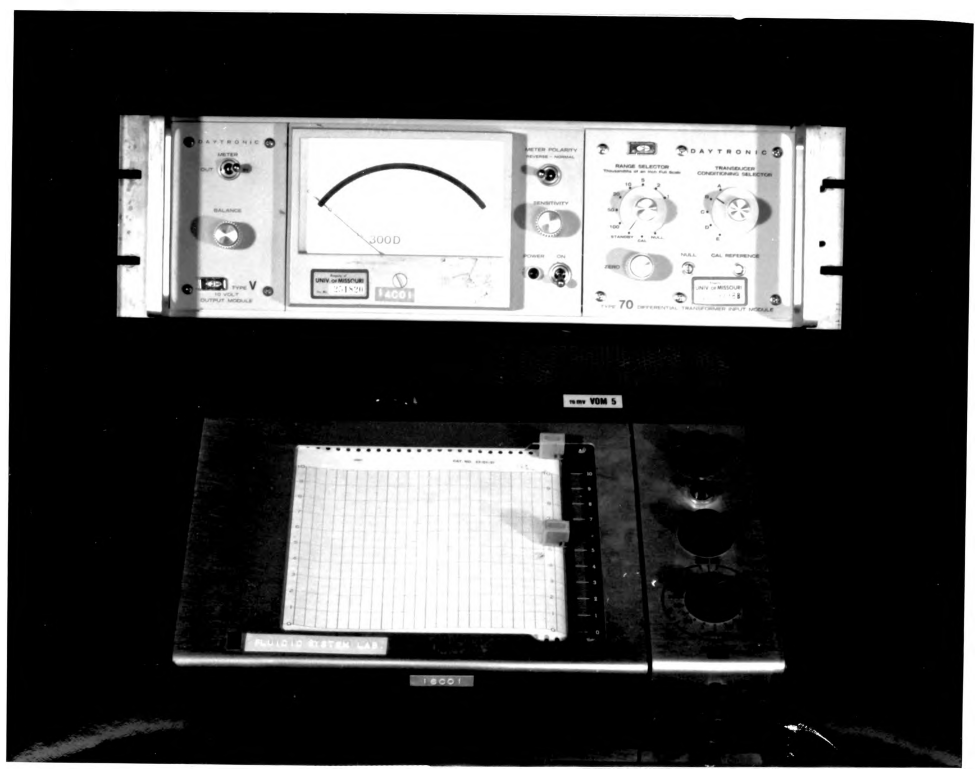

Figure 26. Deformation Recording Equipment

TABLE 6

PARTS LIST FOR ONE STATIC CREEP MACHINE

No. Req'd	Part Name	Dimensions
1	Vertical Support	4"x2"x10" Channel
1	Base Plate	4"x5"x1/2" Steel
1	Support Plate	4 3/4"x8"x1/2" Steel
1	Load Bracket	2"x5 1/2"x1/2" Steel
1	Lever Arm	4"x2"x11 1/2" Channel
2	Lever Arm Support	2 3/8"x7"x1/2" Steel
2	Bushings	1"x1 1/2" Dia. Brass
1	Pivot Axel	1/2"-13x6 1/2"
2	Bracket Bolts	1/4"-20x3"
1	Lead Brick	2"x4"x8" Lead
2	Nuts	1/2"-13
1	Load Indentor	1/2" Dia. x 12" Stainless
2	Ball Bearing Assemblies*	1/2"x1 3/8"(O.D.)-1/2"I.D.
2	Linear Pillow Blocks**	1/2" I.D.
1	LVDT Daytronic+	DS200
1	Daytronic++	300 D-V-70
1	Chart Recorder+++	V.O.M.-5

* Nice, SKF Industries, Inc., Philadelphia, PA

** Thomson, Thomson Industries, Inc., Manhasset, New York

+ Daytronic Corporation, Dayton, Ohio

++ Daytronic Corporation, Dayton, Ohio

+++ Bausch & Lomb, Rochester, New York

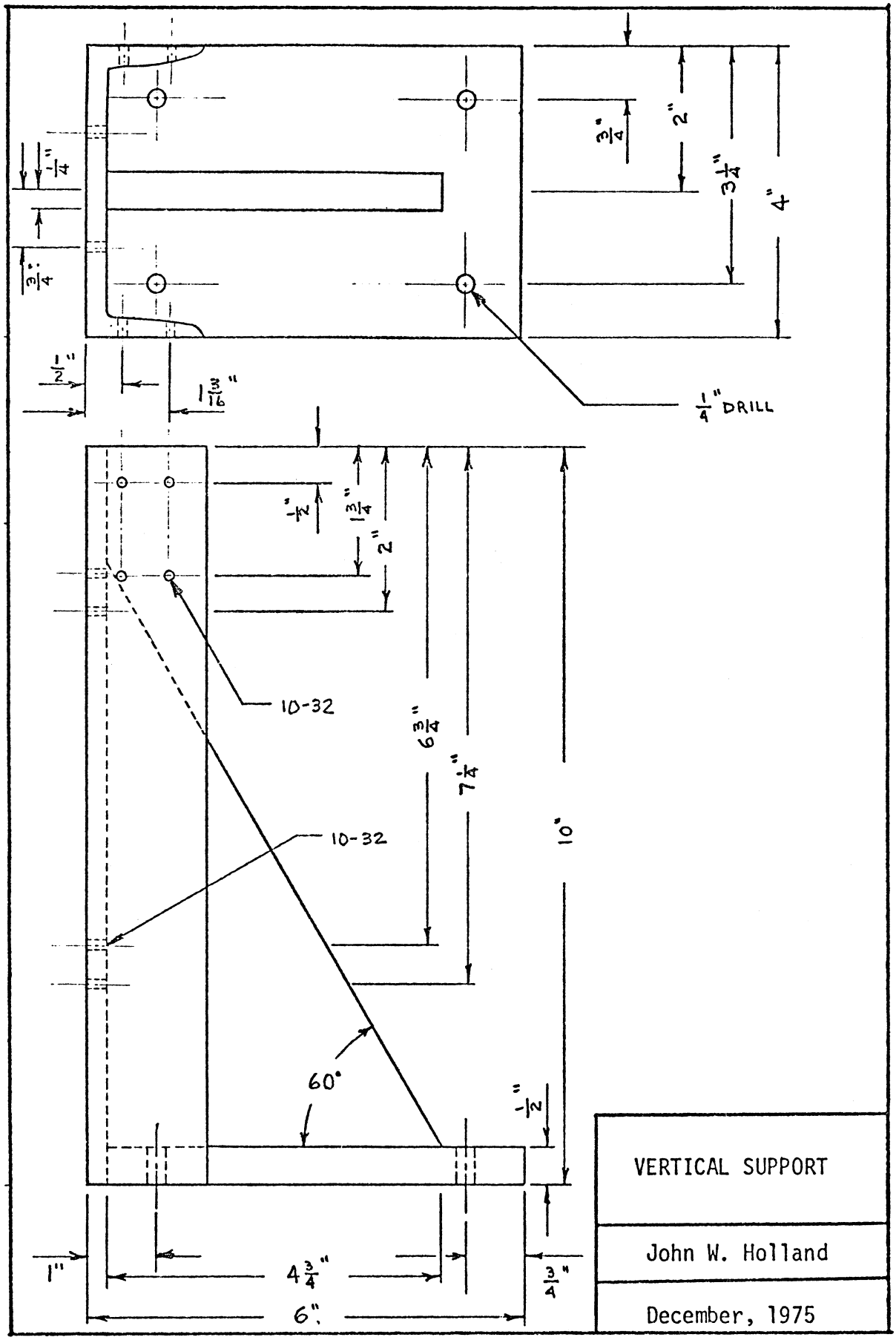

VERTICAL SUPPORT

John W. Holland

December, 1975

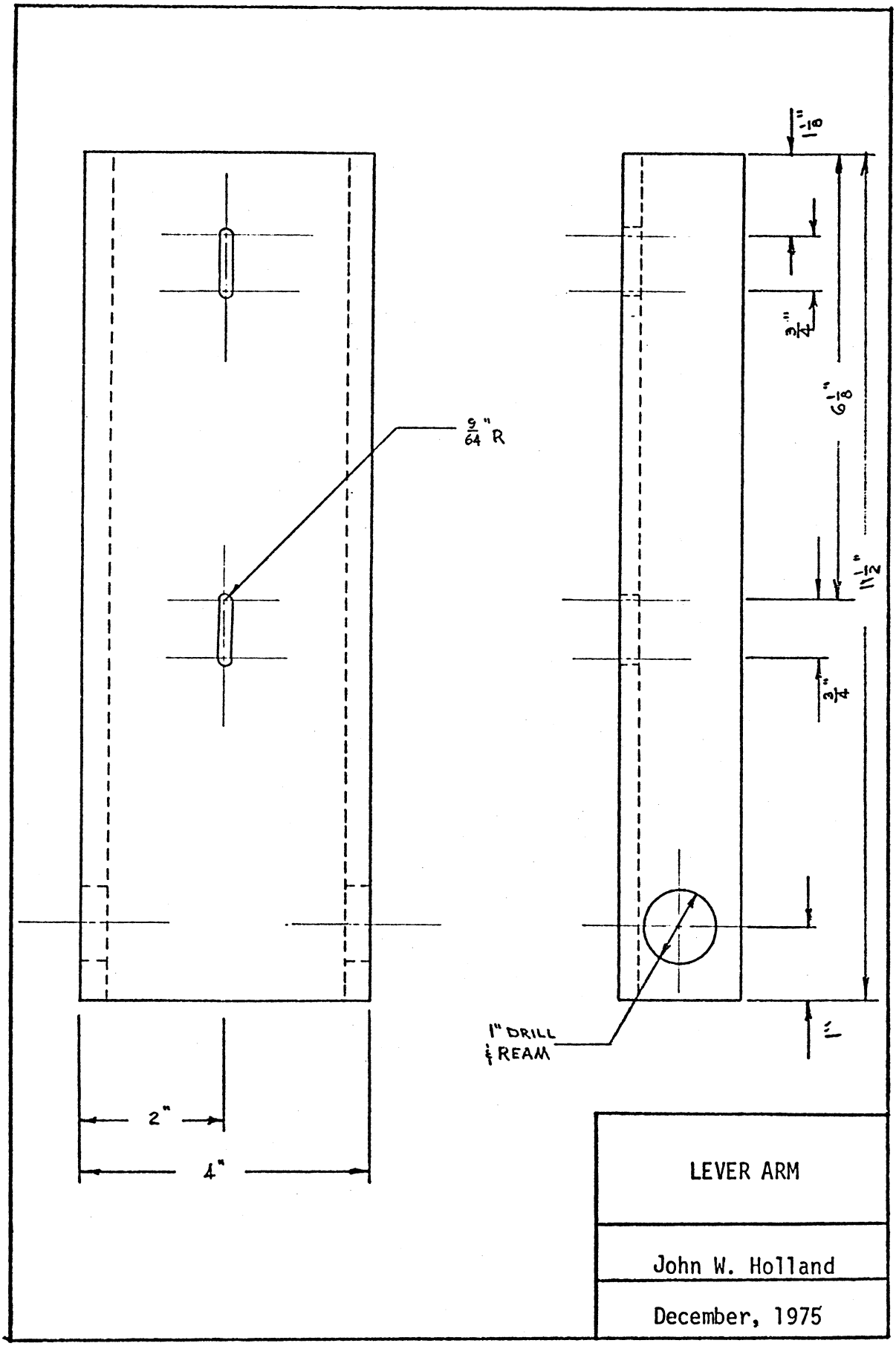

LEVER ARM

John W. Holland

December, 1975

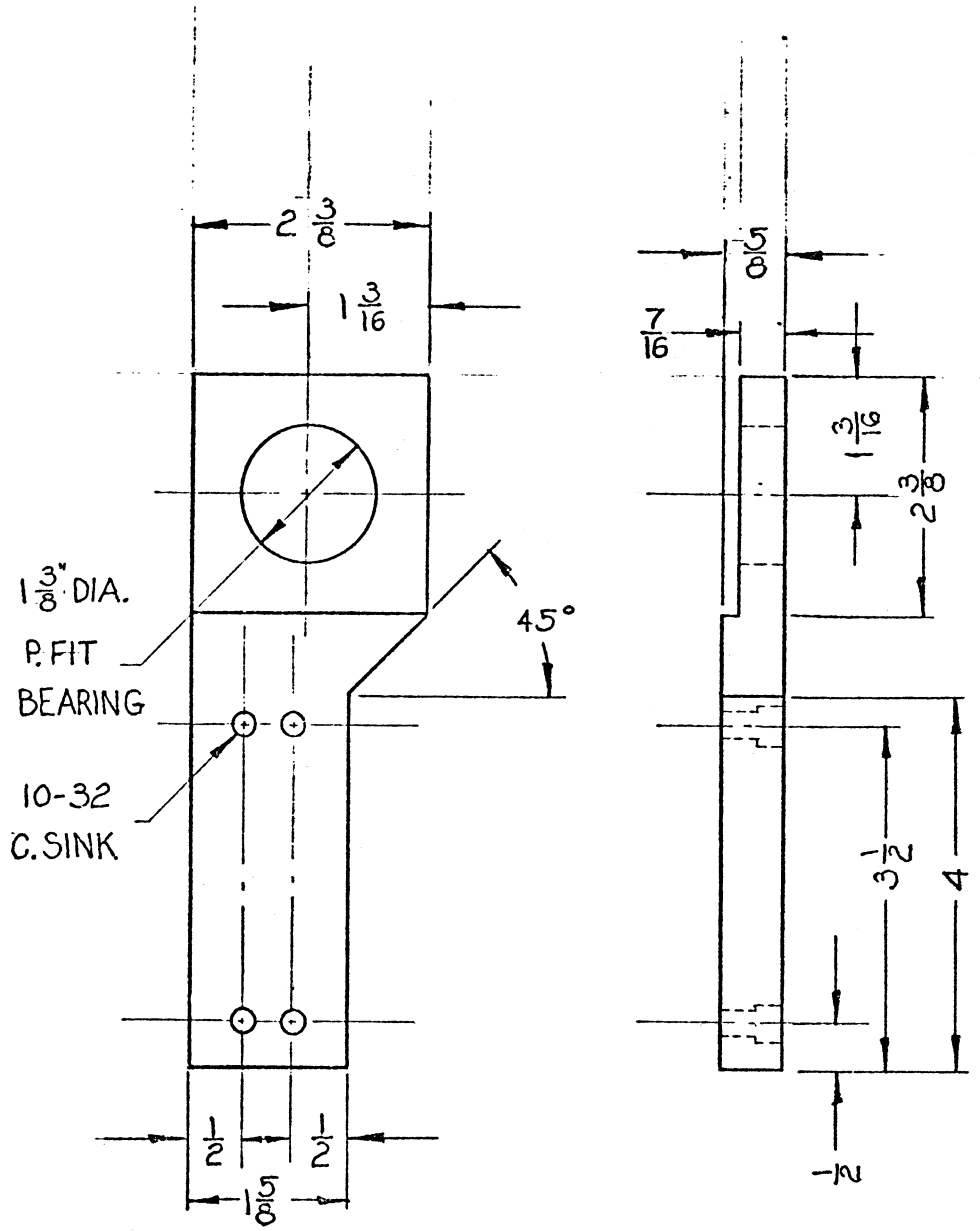

LEVER ARM SUPPORT
John W. Holland
December, 1975

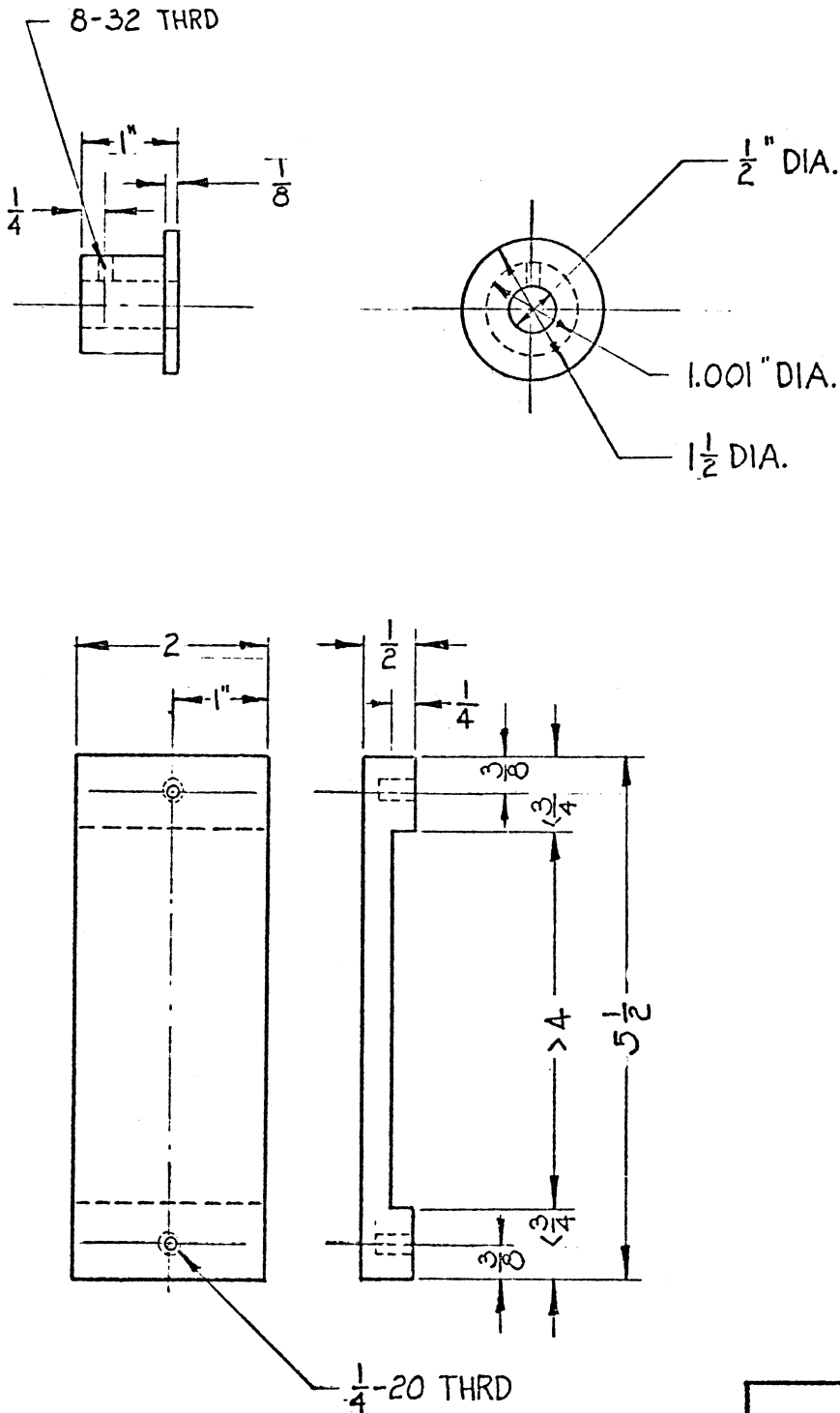

BRASS BUSHING LOAD BRACKET
John W. Holland
December, 1975

APPENDIX B

THEORY OF MICROSTRUCTURAL ANALYSIS EQUIPMENT OPERATION

Ion Microprobe Analyzer

The ion microprobe mass analyzer is one of a new class of instruments developed to provide in-situ mass analysis of a microvolume near the surface of a solid sample. The instrument accomplishes analysis by bombarding the surface with a high energy beam of ions that causes some of the atoms of the surface of the sample to be sputtered away. A fraction of the sputtered particles is electrically charged, and these sputtered ions are collected and analyzed according to their mass-to-charge ratio in a high-transmission double-focusing mass spectrometer. In this way, all materials (oxides, alloys, glasses, etc.) can be analyzed for the iostopes of the elements with a spatial resolution of from 1-300μm and a depth resolution in monolayers. The technique has quite uniform elemental sensitivity throughout the whole mass region and with isotopic detection capability affords use of tracers in diffusion studies.

Electron Microprobe Analyzer

The electron microprobe analyzer, like the ion microprobe, is an instrument capable of chemical analysis of a microvolume of material below the surface of a solid sample. Analysis is accomplished by focusing an electron beam, by electromagnetic lenses, onto the specimen surface.

If the electrons within the beam are of sufficient energy characteristic x-rays will be generated within a microvolume below the specimen surface. Each chemical element may radiate x-rays of specific, known wavelengths termed characteristic x-rays. These wavelengths can be measured by allowing the generated radiation to impinge upon analyzing crystals. The characteristic wavelength can be determined by

measuring the angle of incidence the x-ray beam makes with specific lattice planes, in the analyzing crystal, as diffraction occurs. The crystal planes diffract (i.e., reflect) the x-ray beam when Bragg's Equation is satisfied.

$$\text{Bragg's Law} \quad n\lambda = 2d \sin\Theta$$

The characteristic wavelength (λ) can be calculated from the above mathematical statement of Bragg's Law when the specific lattice spacings (d) and the x-ray angle of incidence (Θ) are both known. Analyzing crystals with different d-spacings are employed to increase the range of characteristic wavelengths which can be analyzed. By comparing the measured values of characteristic wavelengths with tabulated values, most elements within the specimen can be identified.

The intensity of the diffracted x-ray beam is measured by a gas-filled, proportional counter detecting system. The signal from the proportional counter is amplified and electronically analyzed to determine the relative intensity (counts per second) of the diffracted x-ray beam.

The concentration (c), in weight percent, of a specific element within the specimen, can be determined by measuring the intensity of the characteristic radiation from that element in the unknown specimen. This intensity, from the unknown specimen, (Iu) is compared with the intensity (Is) measured for that element in a standard specimen of known composition. Certain corrections must be made so that an accurate concentration value can be determined. These corrections are often labelled ZAF corrections; a computer program used to assess these corrections to microprobe data is discussed in Appendix C. The following

equation can be used to calculate the concentration of a specific element in the specimen:

$$C = \frac{Iu}{Is} \text{ (ZAF) } 100\%$$

Phenomena other than characteristic x-ray generation occur below the specimen surface when the specimen is bombarded with an electron beam. The electrons from the beam, collide with atoms comprising the specimen. Many of these electrons exit the specimen surface following these collisions and are termed backscattered electrons. During many of these collisions, some loosely bound electrons are ejected from their orbitals, and in turn, they may exit the specimen surface. These low energy electrons are called secondary electrons. The quantity of these electrons leaving the specimen is dependent upon the specimen topography. Other electrons, entering the specimen from the bombarding beam, eventually lose much of their energies and are absorbed by the specimen. These electrons contribute to the specimen current of the sample.

The usefulness of these other electron bombardment phenomena can be appreciated following the discussion of another electron microprobe capability. Scanning coils are placed along the electron beam path prior to the specimen surface bombardment. These coils allow the electron beam to sweep across an area upon the specimen surface. An electron beam, in a cathode ray tube, is made to sweep across the tube screen in syncronization with the analyzing electron beam. The intensities of the secondary electrons, the backscattered electrons, and the specimen current can each be measured by various detecting systems. Each of these intensities can separately be displayed on the

cathode ray tube so that their value at each point on the specimen surface can be observed visually.

Images formed on the CRT screen can represent surface topography if the secondary electrons are monitored, or the relative atomic numbers of the phases comprising the analysis area can be displayed if backscattered electrons or the specimen current is monitored. Monitoring of the secondary electrons is the principle of operation for the scanning electron microscope. Imaging of the backscattered electron or specimen current affords easy phase identification if the phases are comprised of elements with adequately different atomic numbers.

X-ray area scans produced from Dispersalloy specimens were illustrated in Chapter III. These photographs were produced by monitoring the characteristic x-ray intensities and displaying them on the CRT screen in an analagous manner to that described for the secondary electrons, etc. Hence, light areas in these micrographs represent areas with concentrations of the specific element being analyzed. As the area of analysis is reduced in size, the magnification of the resulting micrograph is directly increased.

Some electron microprobe analyzers have the capability to electronically position the beam upon the specimen surface, to hold the beam at that spot for chemical analysis, and then to automatically reposition the beam for chemical analysis at another spot. This type of analysis is called a matrix scan. For the diffusion experiment described in Chapter III, the electron beam was repositioned at 80 points along a line across the specimen microstructure. The x-ray intensities of tin, silver and copper were measured, and the data were stored on paper tapes. A computer

program was formulated to correct the intensities, to calculate the chemical compositions and to plot the concentrations as functions of position along the line of analysis. These data plots are illustrated in Appendix D.

Tables 7 and 8 contain the electron microprobe adjustments used for these particular experiments.

TABLE 7

ELECTRON BEAM CONTROL ADJUSTMENTS

Accelerating Potential	15 KV
Filament Current	150 μamperes
Beam Current	0.2 μamperes

TABLE 8

SPECTROMETER ADJUSTMENTS

X-ray Line	Spec. No.	Analyzing Crystal
Tin Lα	1	ADP
Silver Lα	2	ADP
Cu Lα	3	RAP
Hg Mα	1	ADP

The concentration values tabulated in Chapter III represent the averages of ten individual intensity counts at each analysis point. Each x-ray intensity count was measured for ten seconds. X-ray background counts were performed at each point in a similar manner to the intensity counts. Background counts are produced by adjusting the analyzing

spectrometers to positions slightly away from those required for measuring the characteristic wavelengths. These background counts are essential for accurate chemical analysis, and they are required for use in the correction program discussed in Appendix C.

Scanning Electron Microscope

The theory of operation of the scanning electron microscope (SEM) was briefly discussed in the prior section of this Appendix. An electron beam scanning the specimen surface and an electron beam scanning a CRT screen are caused to traverse their relative areas in sycronization. The intensity of the secondary electron exiting the specimen surface are detected and displayed by the CRT screen. Hence, the intensity of secondary electrons, exiting the specimen at a particular spot, is simultaneously displayed at a corresponding spot on the CRT screen. Since the quantity of secondary electrons being generated is related to the surface topography, the image displayed on the CRT screen is a representation of the surface topography.

Resolution of submicroscopic details can be accomplished by the SEM; the quality of resolution is dependent upon the electron beam diameter. Due to the imaging technique, the SEM can attain greater depths of field than possible in optical microscopes. The SEM is useful in studying rough, uneven surfaces at high magnifications.

APPENDIX C

ELECTRON MICROPROBE X-RAY INTENSITY CORRECTION PROGRAM FOR ACCURATE CHEMICAL COMPOSITION DETERMINATION

There are a number of computer programs available for converting raw microprobe x-ray intensities into chemical composition. Many microprobe operators have concluded that MAGIC* was one of the most generally applicable correction programs. MAGIC is an acronym for Microprobe Analysis General Intensity Corrections. It has achieved rather widespread usage and has been modified by the various users for many different computers, including the CDC, GE, Honeywell, PDP-11, and Burroughs computers. The program has been continually updated to take into account newer correction techniques. As a consequence of the updating, MAGIC was reprogrammed in Fortran IV for use on an IBM 360 computer in 1968. Additional modifications have been made to the MAGIC program, and version IV is now in usage.

All data are corrected for dead time, background, absorption and atomic numbers. If fluorescence is present, the data are corrected for that phenomenon also. The dead time refers to the time that the x-ray proportional counter cannot detect radiation due to the slow dissipation of an ion sheath formed in the vicinity of the counter anode. The dead time is on the order of a microsecond. The background refers to that measured intensity not attributable to the particular characteristic radiation under analysis. Sources of background intensity are varied (e.g., counting electronics).

Two factors effect the absorption of x-rays. First, an alloy has a different absorption coefficient than does a standard. Second, the electron distribution of an alloy is different than for a standard;

---

* MAGIC, J. W. Colby, 4th Material Conference on Electron Microprobe Analysis, 1969.

therefore the characters of the paths the x-rays traverse in the alloy are different than for the standard. The atomic number effect is responsible for the second contribution to the absorption effect.

The atomic number effect results because fewer backscattered electrons are formed from a low mean atomic number alloy. Also, electrons lose energy more rapidly in the alloy, and therefore they have less opportunity to produce ionizations and thus generate fewer x-rays. The result of these two factors is that the generated intensity ratio is less than the expected mass ratio for a high atomic number element in a lower mean atomic number alloy.

The fluorescence effect will occur when the characteristic x-rays of some alloy components eject core electrons of other alloy components, thus creating fluorescent radiation. The radiation detectors cannot differentiate between the characteristic and fluorescent radiation sources. In an analagous manner, radiation from the continuous spectra can also generate fluorescent radiation.

A paper presented by J. W. Colby, MAGIC IV - A COMPUTER PROGRAM FOR QUANTITATIVE ELECTRON MICROPROBE ANALYSIS (7th Material Conference on Electron Microprobe Analysis, 1972), indicates the particular equations employed to correct the x-ray intensity data. In the Appendix of Colby's paper, a reprint of the Fortran IV correction program is tabulated. Also, examples of typical input and output are included.

APPENDIX D

MATRIX LINE SCAN DATA

PLOTS OF AGED DISPERSALLOY

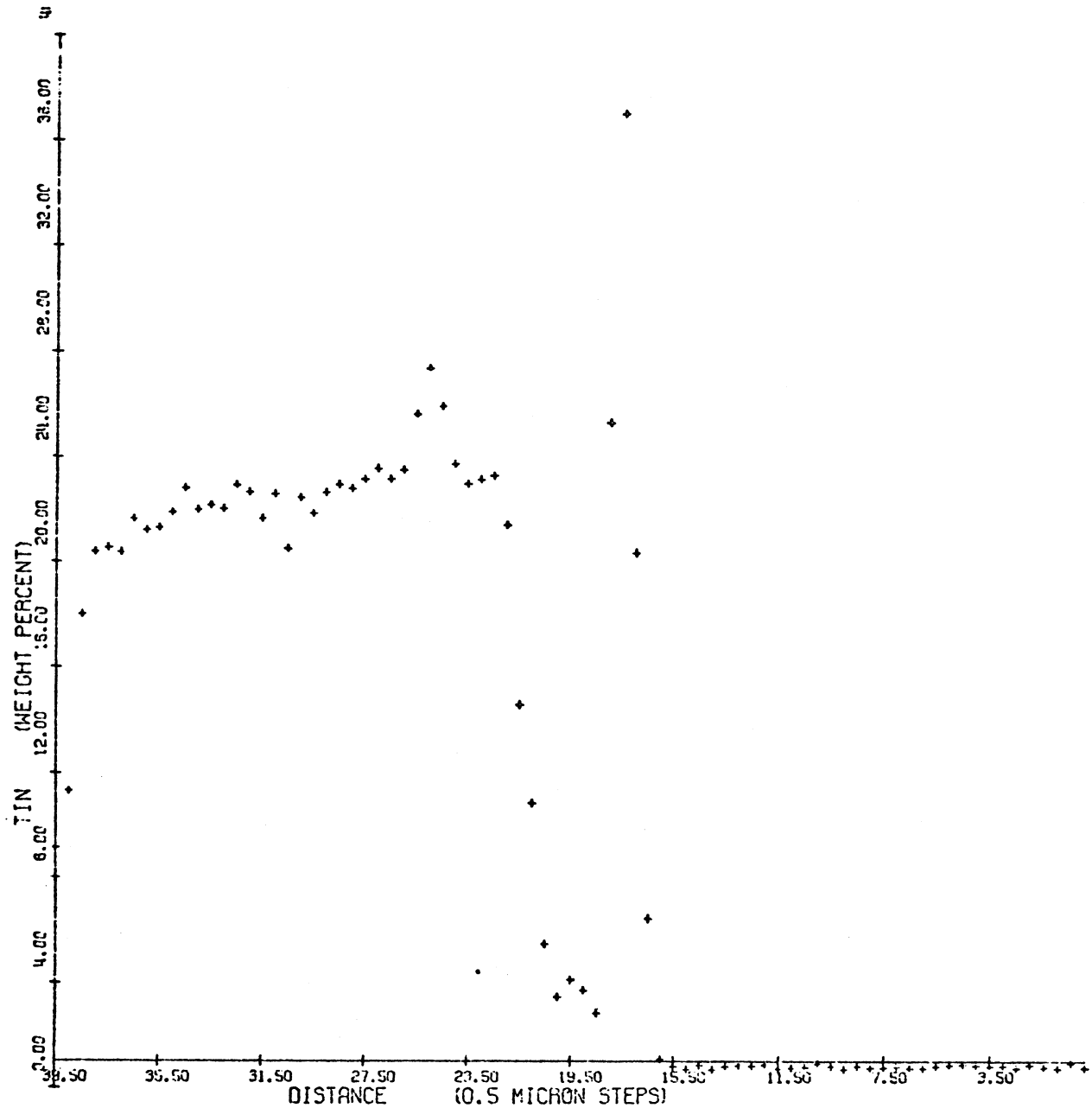

Figure 27. Variabtion in Tin Concentration Across a One Day Dispersalloy Specimen

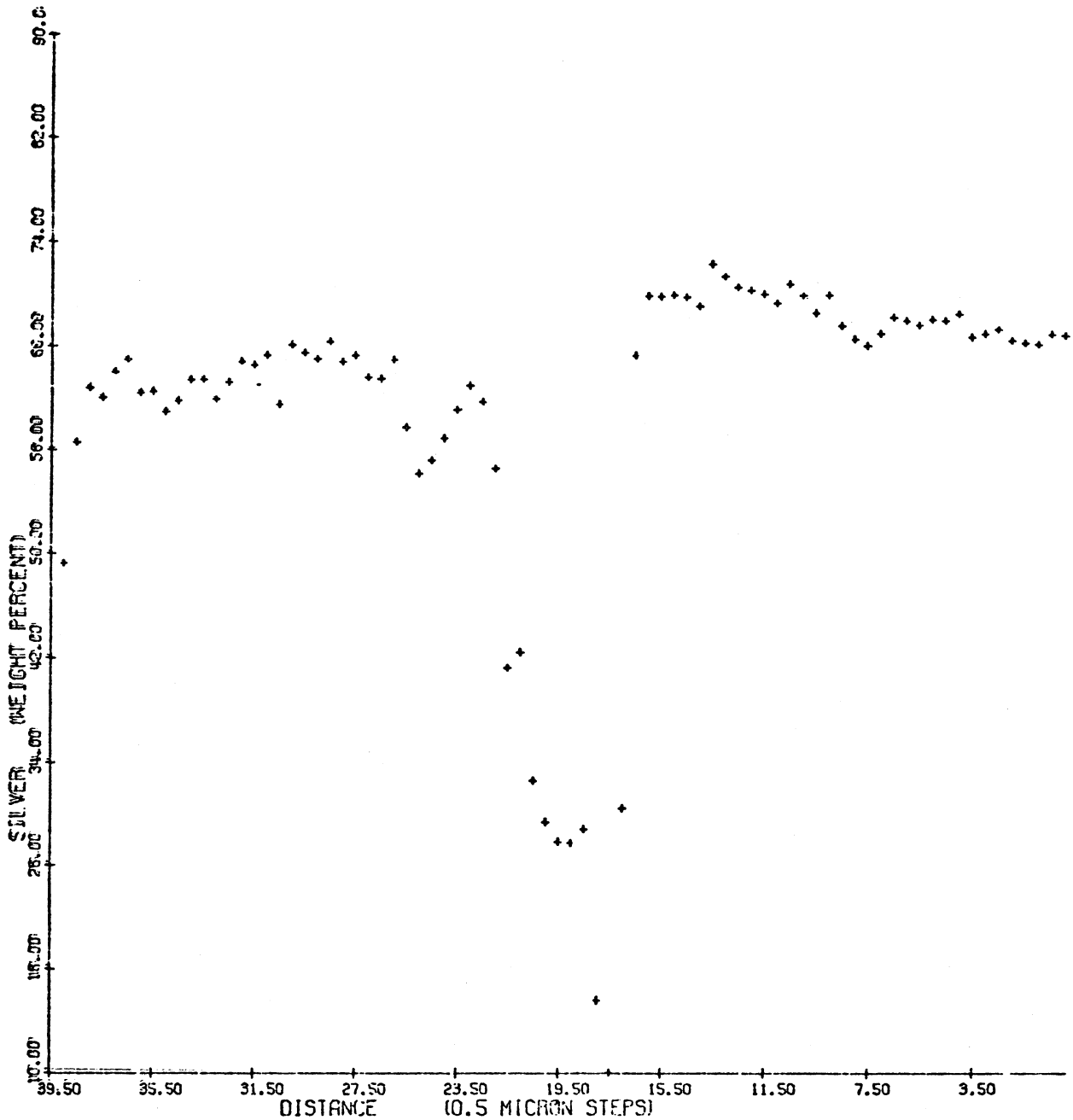

Figure 28. Variation in Silver Concentration Across a One Day Dispersalloy Specimen

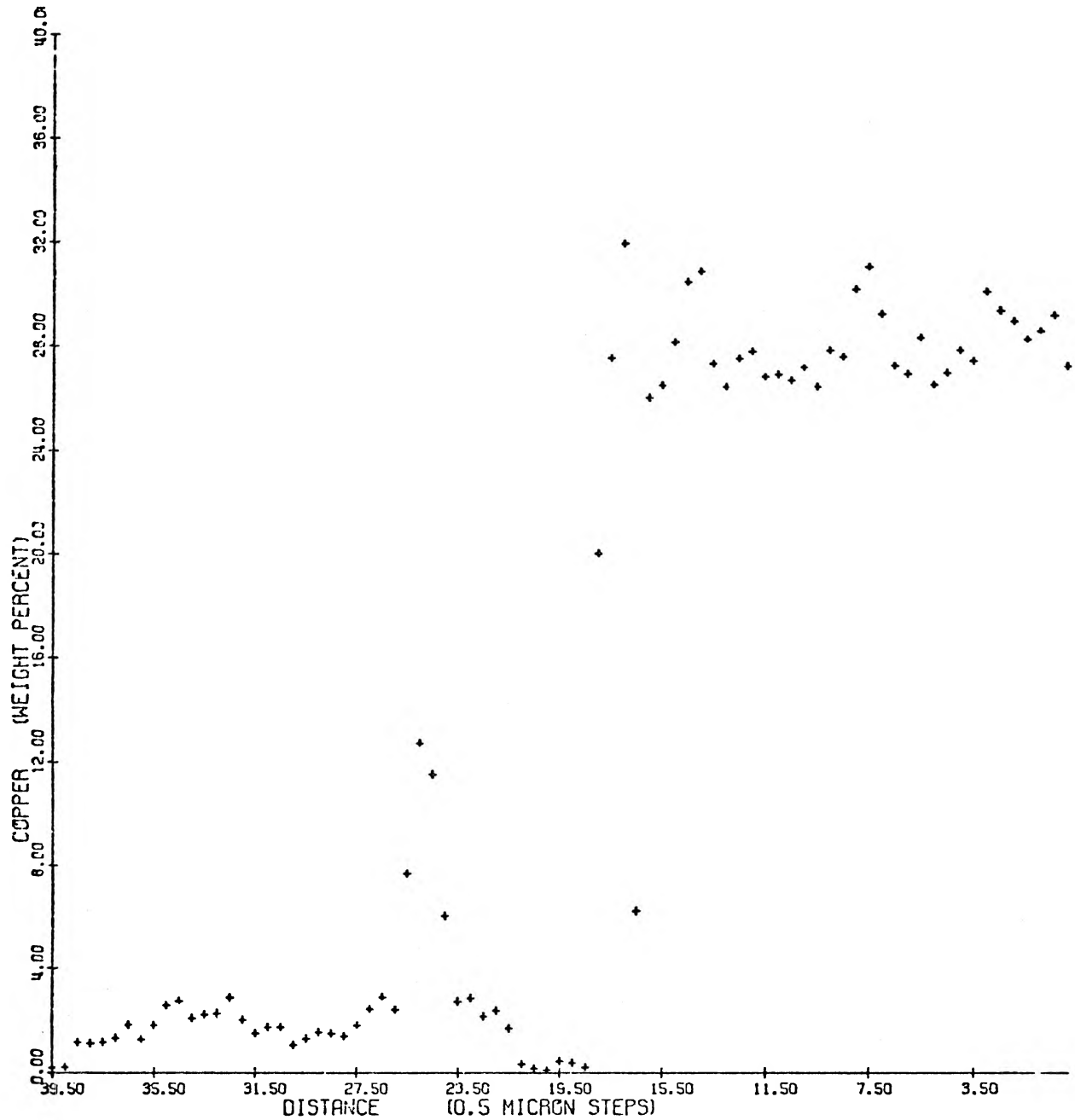

Figure 29. Variation in Copper Concentration Across a One Day Dispersalloy Specimen

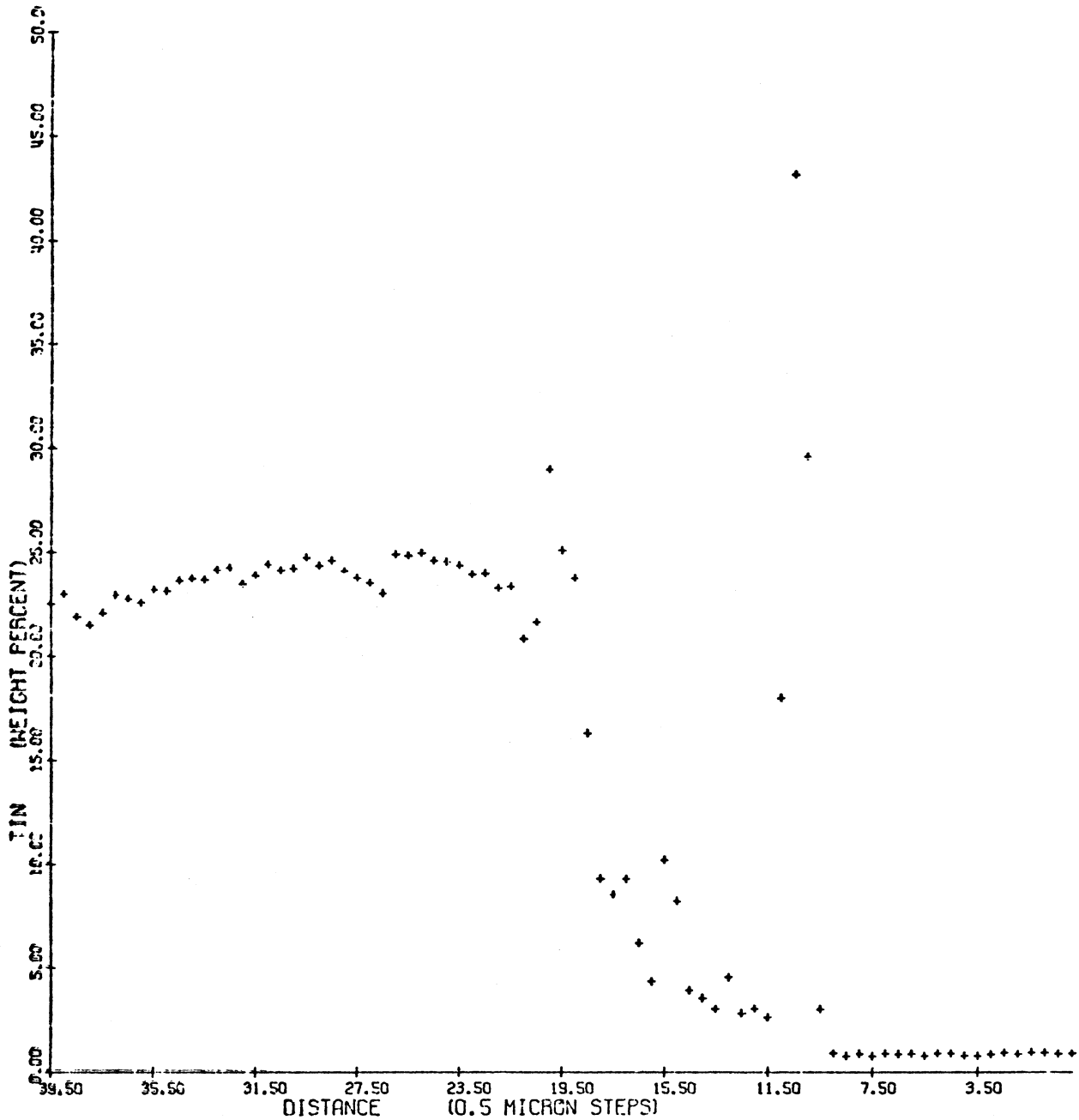

Figure 30. Variation in Tin Concentration Across a Four Day Dispersalloy Specimen

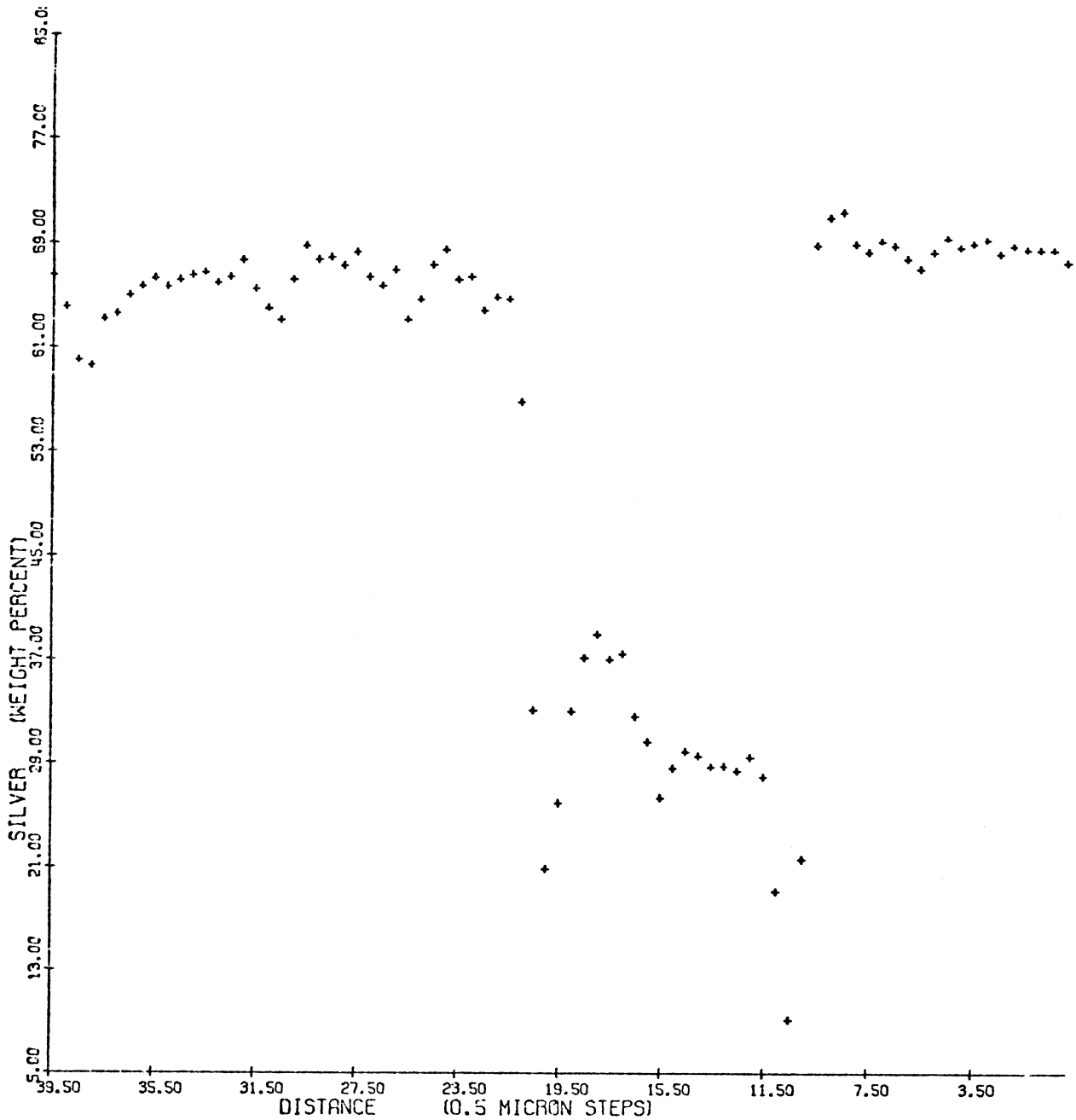

Figure 31. Variation in Silver Concentration Across a Four Day Dispersalloy Specimen

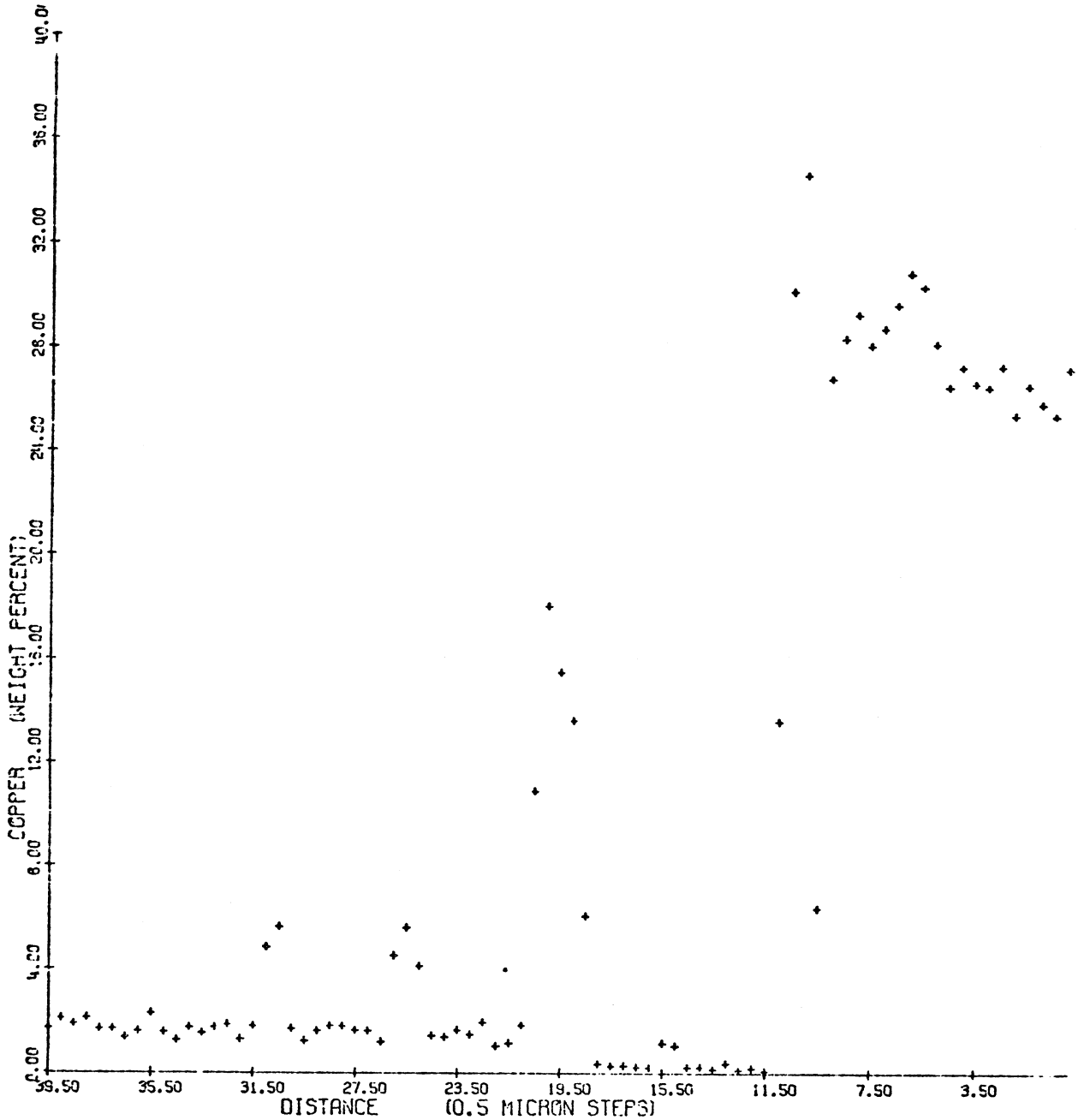

Figure 32. Variation in Copper Concentration Across a Four Day Dispersalloy Specimen

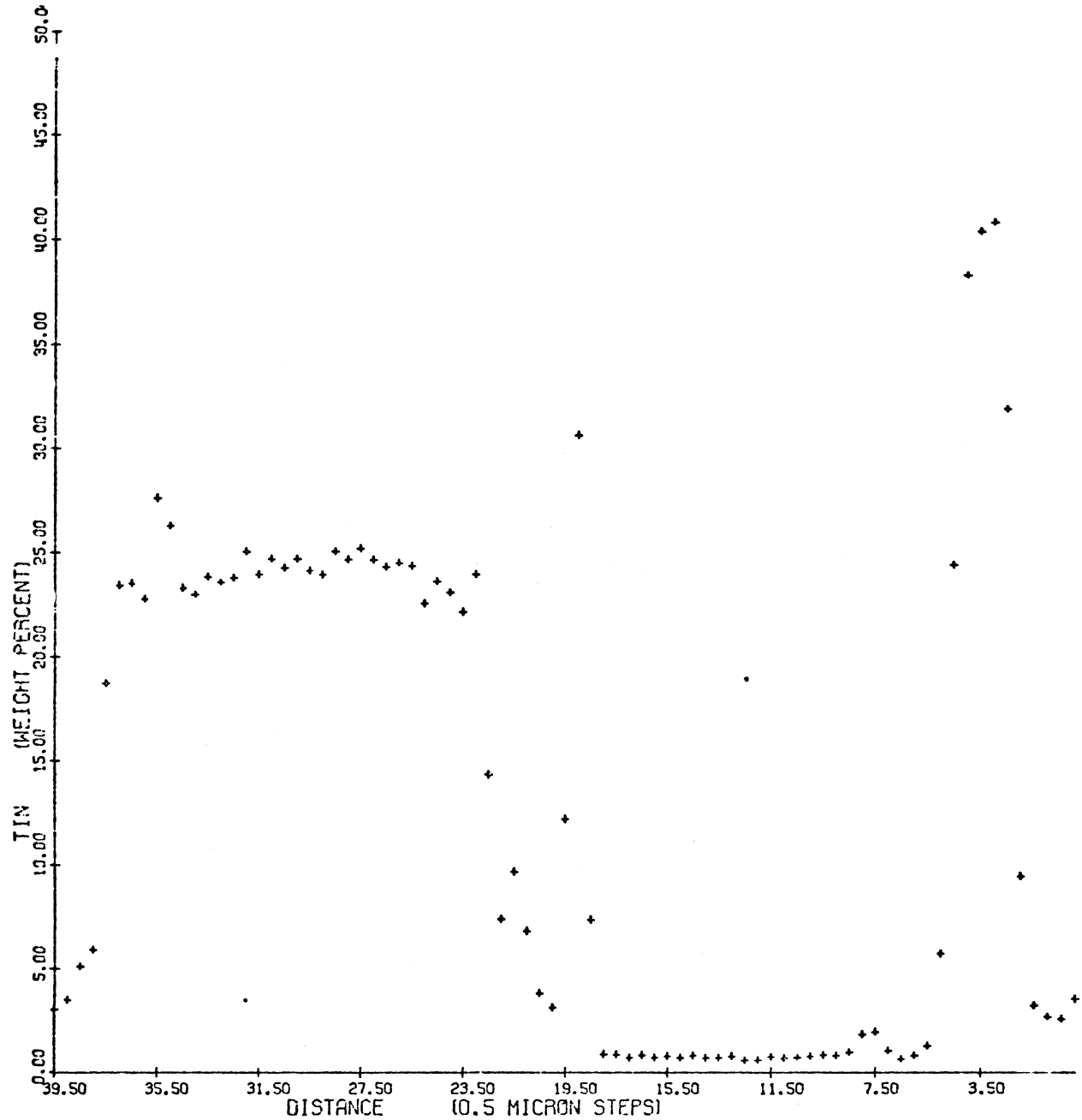

Figure 33. Variation in Tin Concentration Across a Seven Day Dispersalloy Specimen

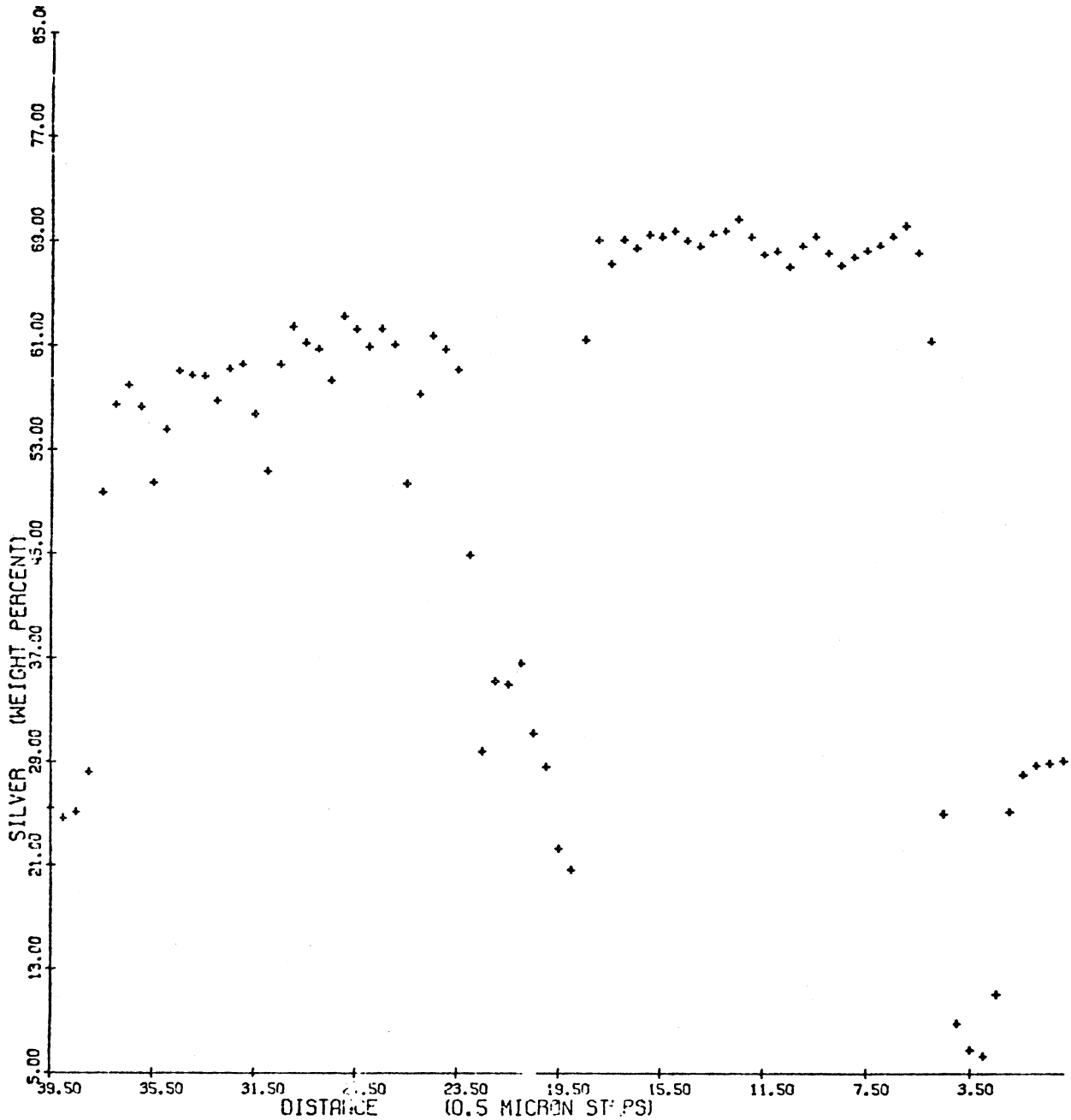

Figure 34. Variation in Silver Concentration Across a Seven Day Dispersalloy Specimen

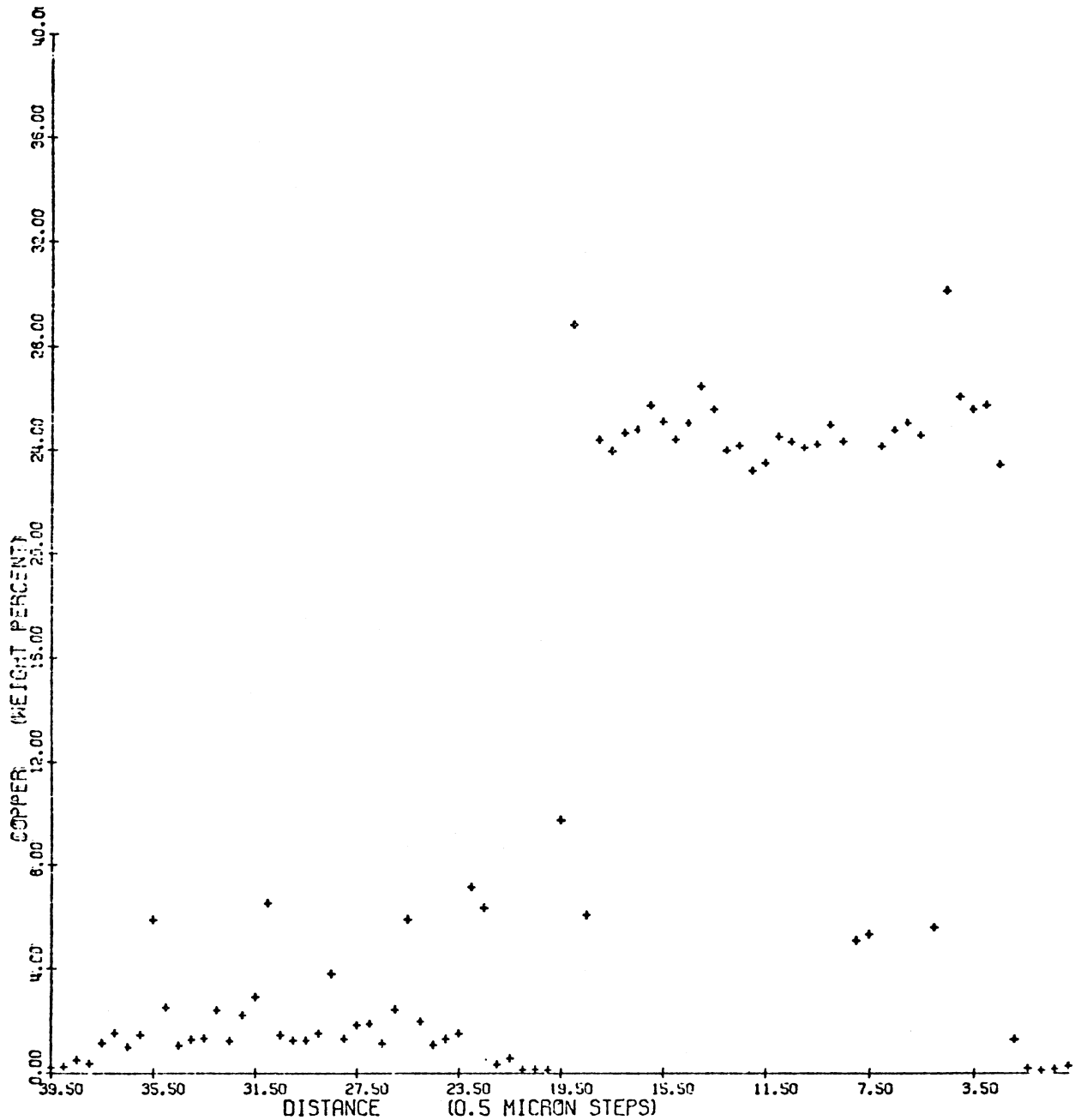

Figure 35. Variation in Copper Concentration Across a Seven Day Dispersalloy Specimen

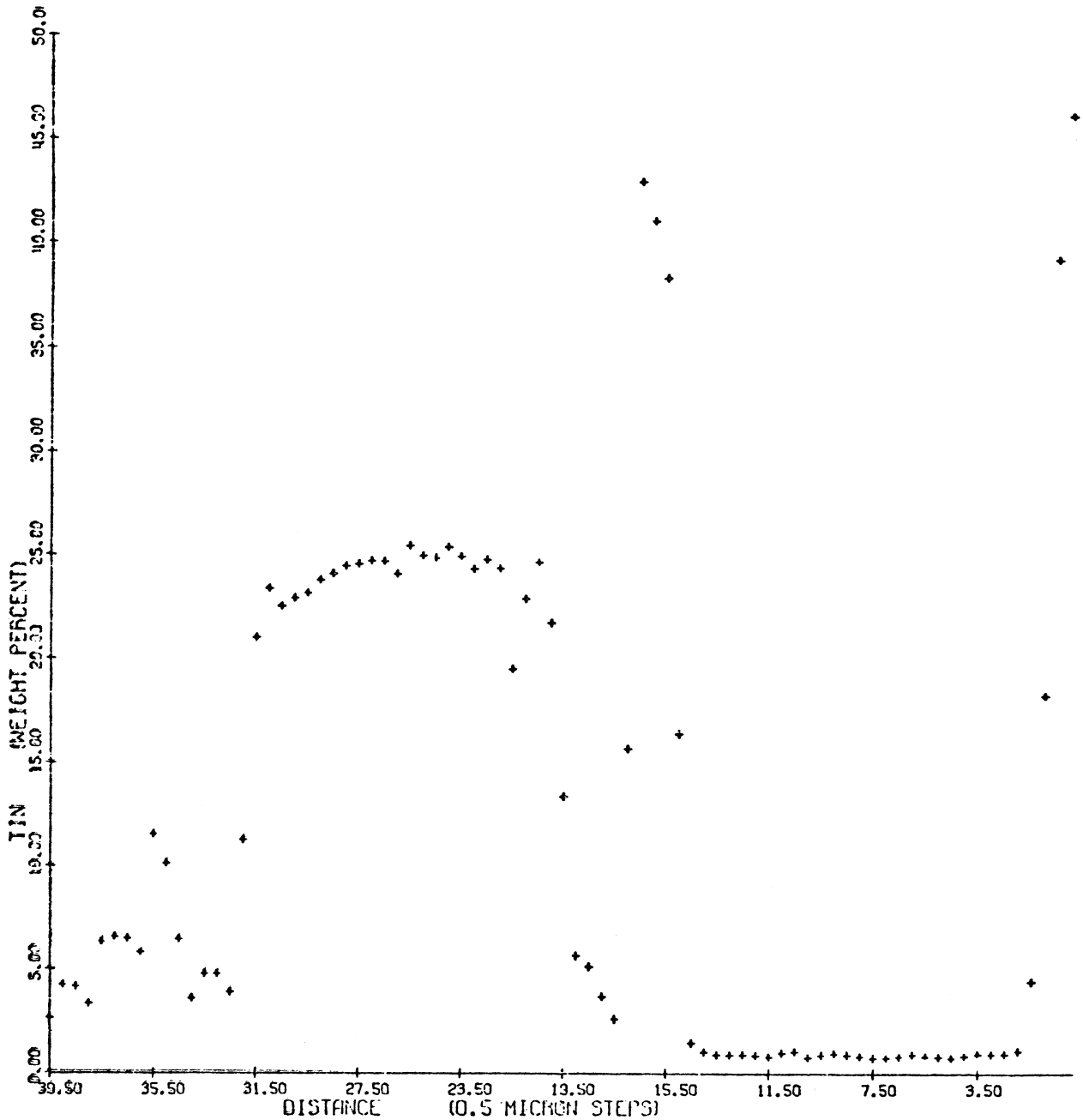

Figure 36. Variation in Tin Concentration Across a Fourteen Day Dispersalloy Specimen

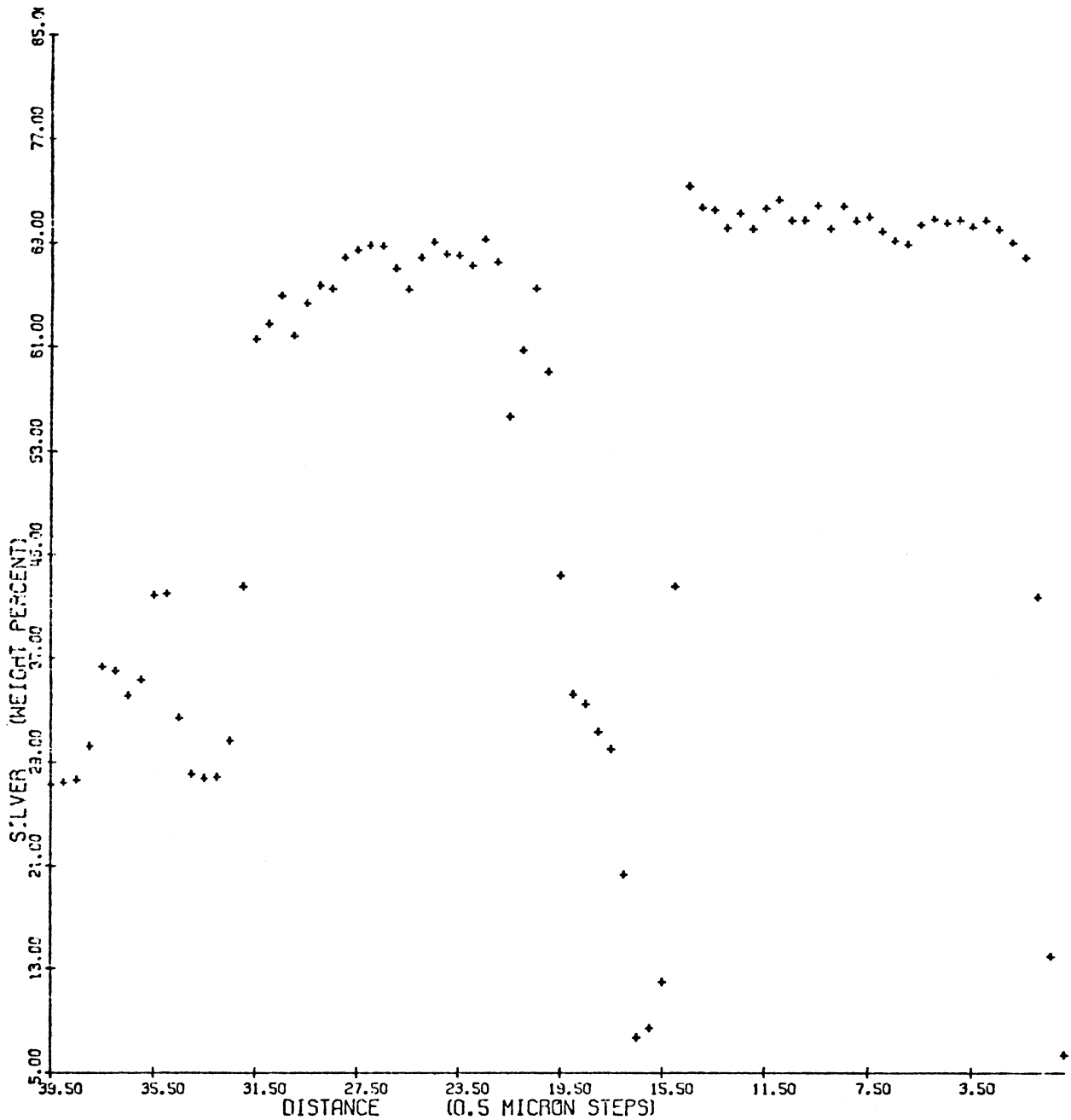

Figure 37. Variation in Silver Concentration Across a Fourteen Day Dispersalloy Specimen

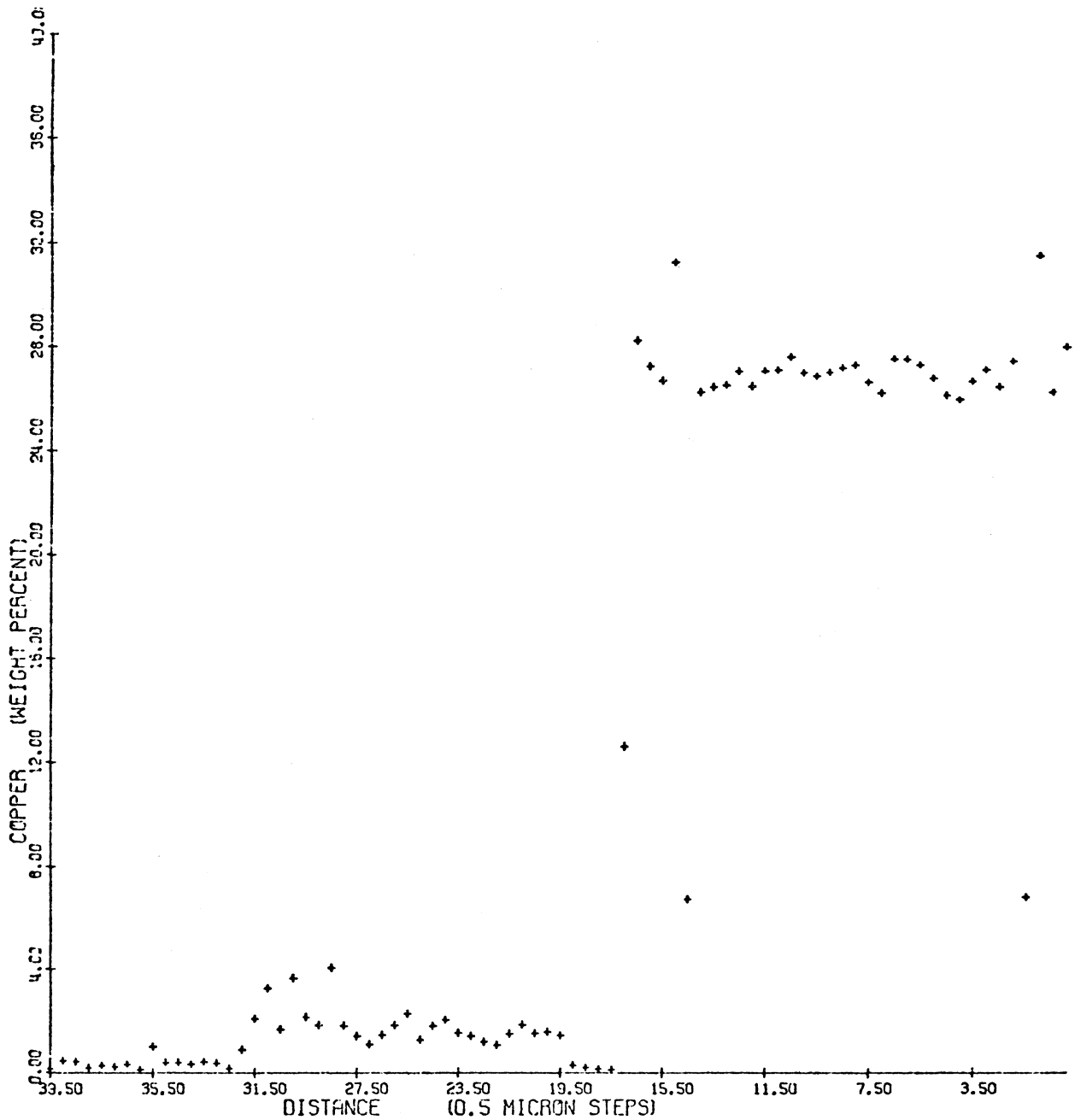

Figure 38. Variation in Copper Concentration Across a Fourteen Day Dispersalloy Specimen

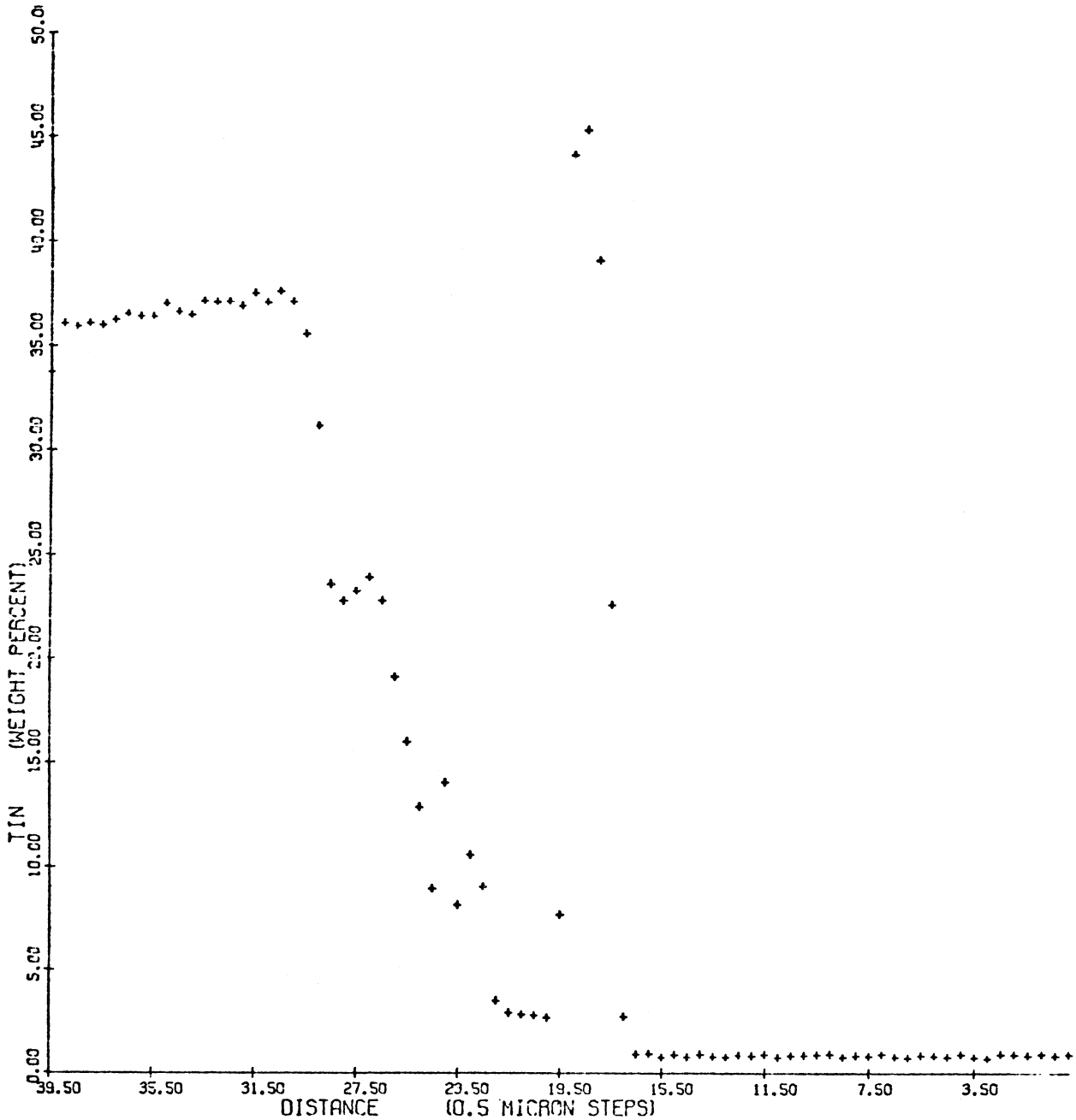

Figure 39. Variation in Tin Concentration Across a Twenty-One Day Dispersalloy Specimen

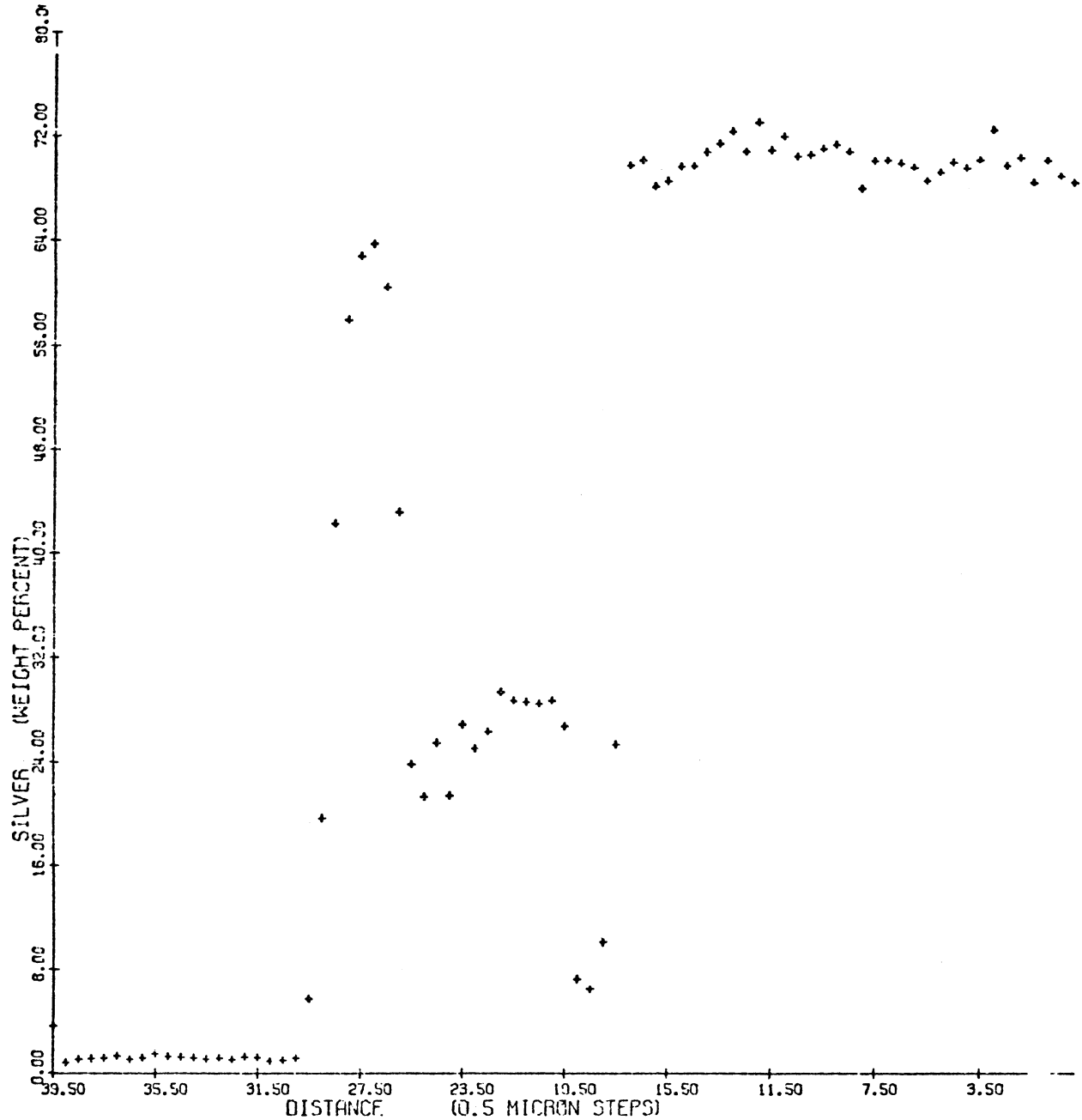

Figure 40. Variation in Silver Concentration Across A Twenty-One Day Dispersalloy Specimen

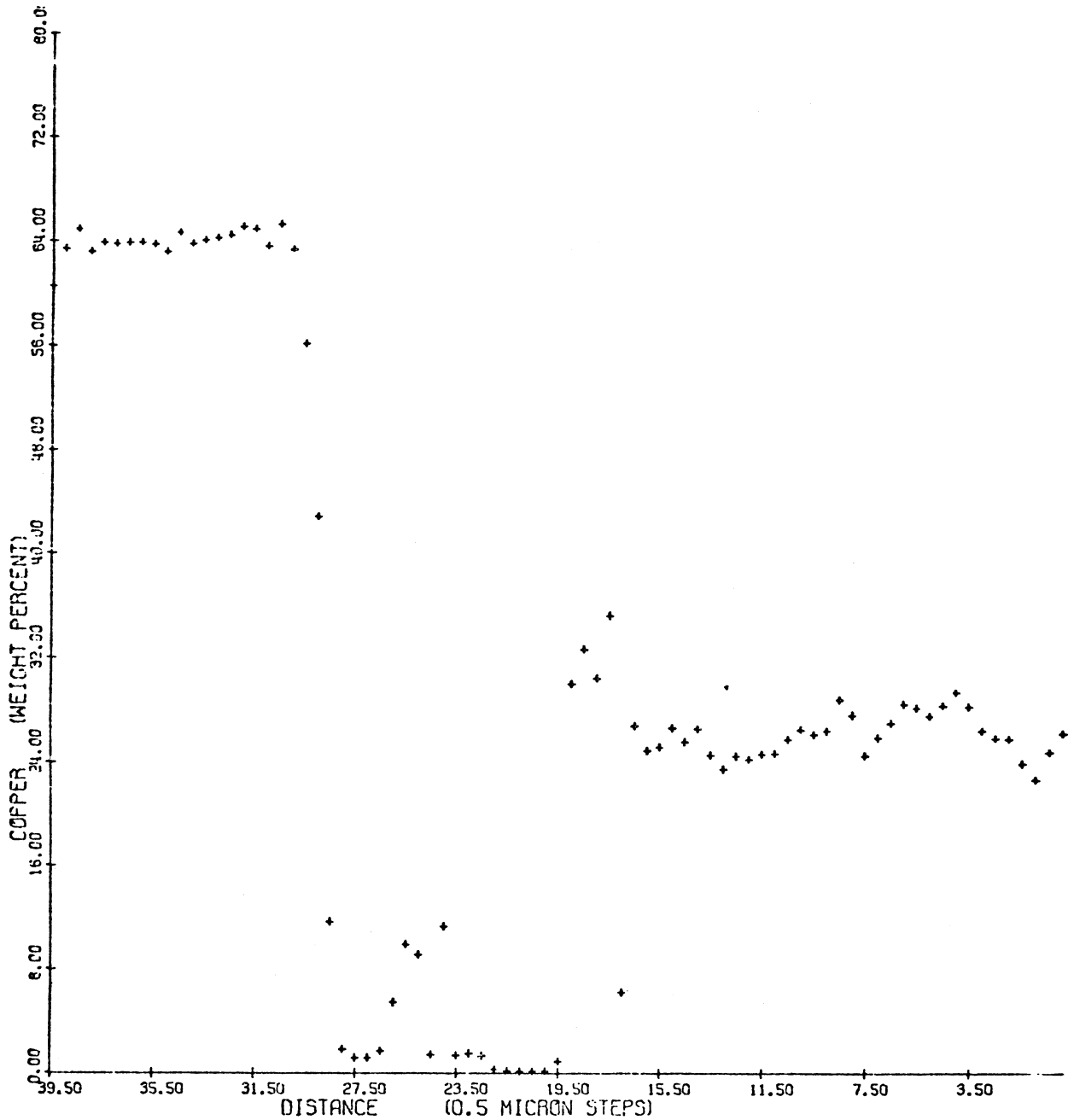

Figure 41. Variation in Copper Concentration Across a Twenty-One Day Dispersalloy Specimen

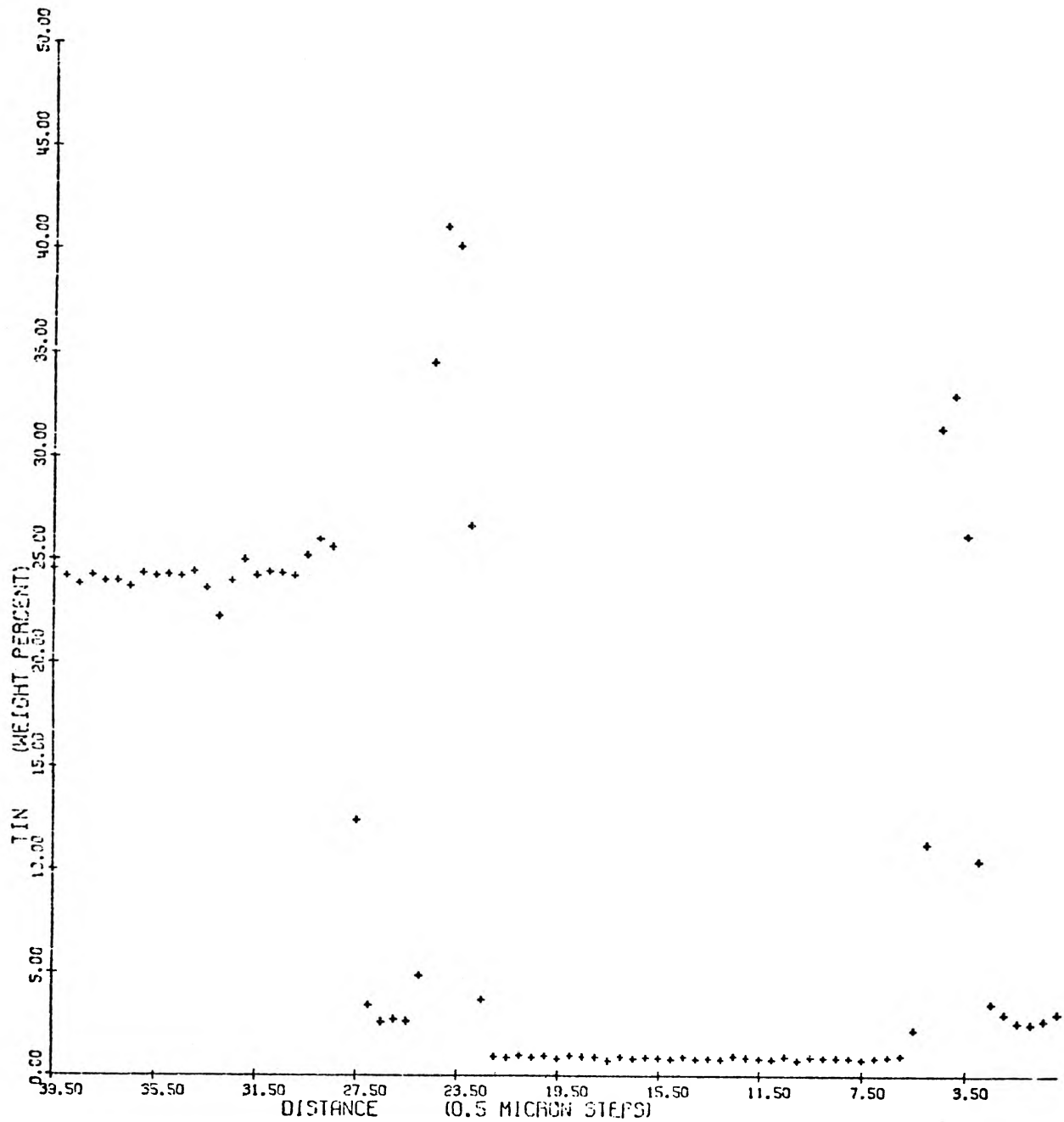

Figure 42. Variation in Tin Concentration Across a Twenty-Eight Day Dispersalloy Specimen

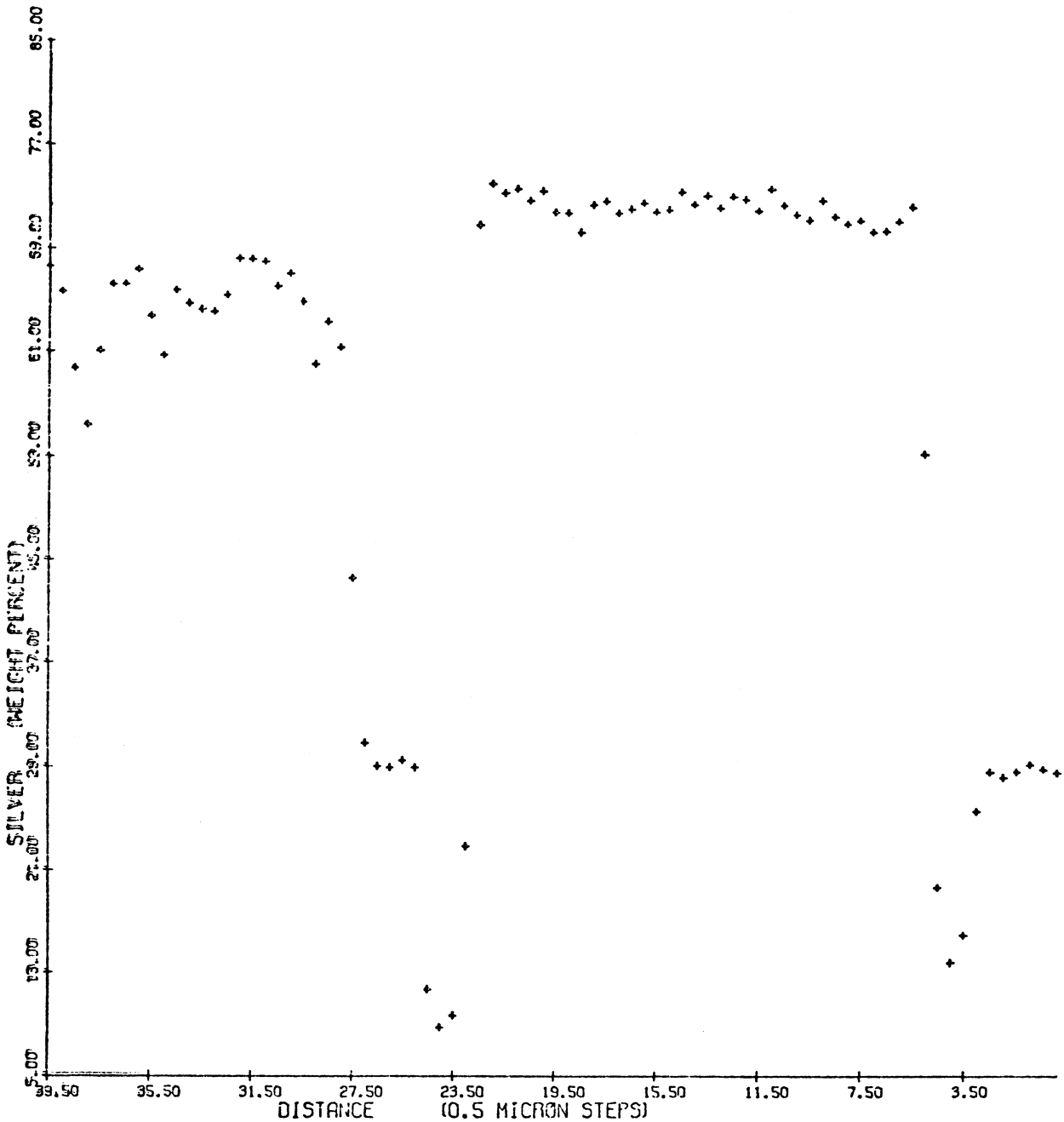

Figure 43. Variation in Silver Concentration Across a Twenty-Eight Day Dispersalloy Specimen

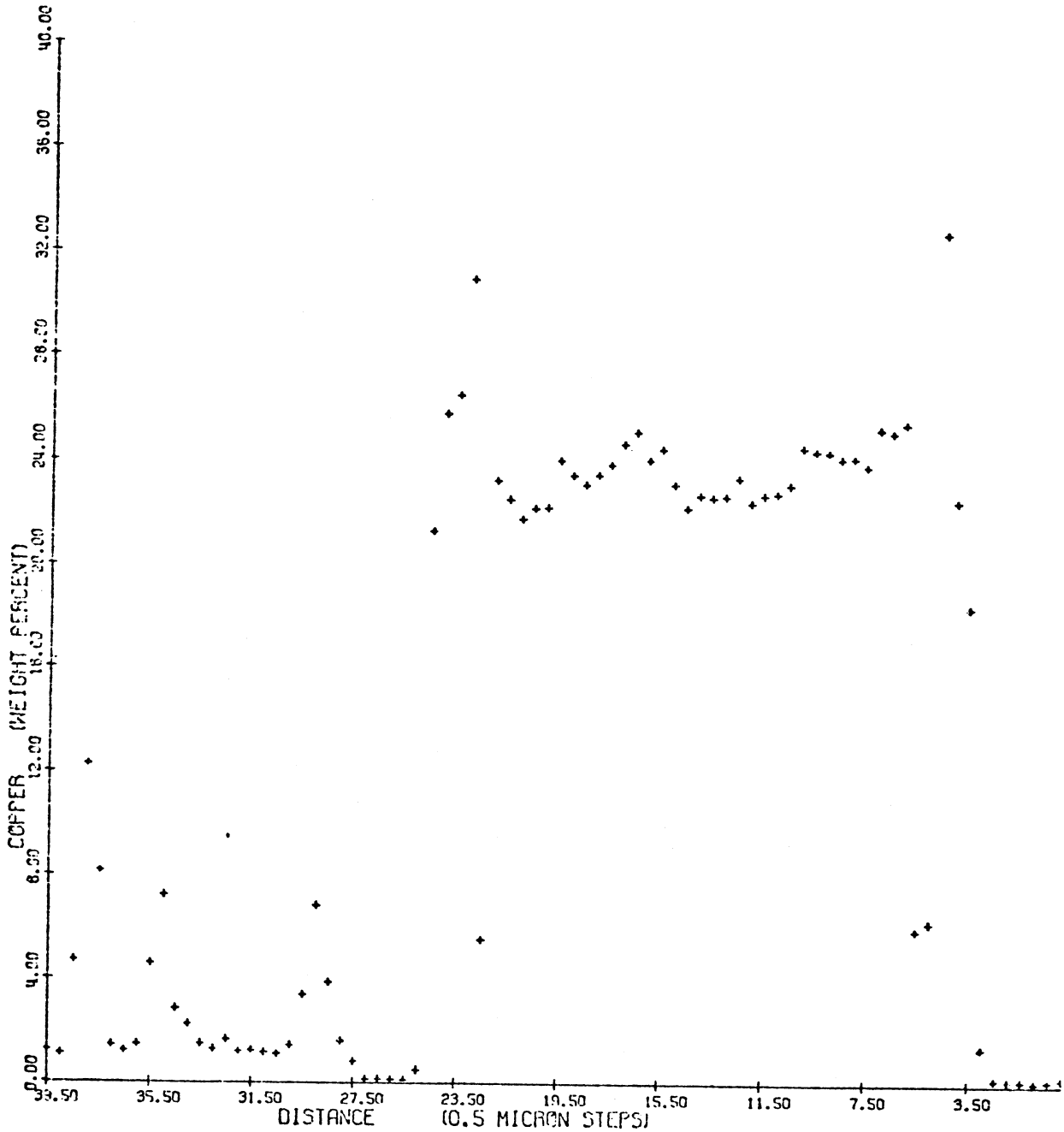

Figure 44. Variation in Copper Concentration Across a Twenty-Eight Day Dispersalloy Specimen

REFERENCES

1. American Dental Association Specification No. 1 for Dental Amalgam, in Guide to Dental Materials and Devices, 5th ed., Chicago: American Dental Association, 1970.

2. Asgar, Kamal and Sutfin, Lloyd, J. Dent. Res., 44, 977. 1965.

3. Burdekin, D. A. and Gibbs, J. N., Nature, 240, 304. 1972.

4. Constitution of Binary Alloys, 2nd Edition, New York, McGraw-Hill. 1958.

5. Greener, E. H. and Sarkar, N. K., "Corrosion Resistance of New Dental Alloys," 49th General Session of the IADR, Chicago, Illinois, 1971.

6. Guthrow, C. Earl, Johnson, Lewis B., and Lawless, Kenneth R., J. Dent. Res., 46, 1372. 1967.

7. Hansen, D. A., Holland, J. W., Lewis, S. A., and Moore, D., J. Biomed. Mat. Res., ,

8. Holland, John W., Masters Thesis: University of Missouri-Columbia, 1972.

9. Innes, D. B. K. and Youdelis, W. V., J. Canada Dent. A., 29, 587, 1963.

10. Johnson, L. N., J. Dent. Res., 51, 789-794. 1972.

11. Jorgenson, Knud Dreyer, Acta Odont, Scand., 23, 347. 1965.

12. Jorgenson, Knud Dreyer and Saito, Tsuyoshi, Acta Odont. Scand., 28, 129. 1970.

13. Lewis, Stephen A., Masters Thesis: University of Missouri-Columbia, 1972.

14. Mahler, D. B., J. Dent. Res., 37, 516-26. 1958.

15. Mahler, David B. and Van Eysden, Jan, J. Dent. Res., 48, 501-508. 1969.

16. Mahler, David B., Terkla, Louis G., Van Eysden, Jan, and Reisbick, Morris H., J. Dent. Res., 49, 1452-1457. 1970.

17. Mahler, D. B., Adey, J. D. and Van Eysden, J., J. Dent. Res., 52, 74-78. 1973.

18. Mahler, D. B., Adey, J. D. and Van Eysden, J., J. Dent. Res., 54, 218-226. 1975.

19. Marek, M. and Hochman, R. F., "The Corrosion Behavior of Dental Amalgam Phases as a Function of Tin Content," 51st General Session of the IADR, Washington, D.C., 1973.

20. Marek, M., Hochman, R. F., and Butler, M. F., "Crevice Corrosion in Dental Amalgam Restorations," 51st General session of the IADR, Washington, D. C., 1973.

21. Marek, M., Private Communication, University of Georgia, 1974.

22. Mateer, Richard S. and Reitz, Clair D., J. Dent. Res., 49, 339. 1970.

23. Mateer, Richard S. and Reitz, Clair D., J. Dent. Res., 51, 1546. 1972.

24. Moore, David L. and Stewart, Jack L., J. Pros. Dent., 17, 372. 1967.

25. Moser, David, Private Communication, University of Missouri-Columbia, 1974.

26. Paffenbarger, G. C. and Hoeppner, D. W., Int. Dent. J., 16, 450. 1966.

27. Pires, Jose A. F., Hodson, Jean T., Scott, William D., Stibbs, Gerald D., J. Pros. Dent., 22, 2340240. 1969.

28. Seino, S., J. Jap. Res. Soc. Dent. Mat. Appl., 15, 25-33. 1966.

29. Skinner, E. W. and Phillips, R. W., The Science of Dental Materials, 298, W. B. Saunders, 1967 (Ed. 6).

30. Stoner, G. E., Lawless, K. R. and Wawner, F., J. Dent. Res., 50, 519. 1971.

31. Terkla, L. G. and Mahler, D. B., J. Dent. Res., 43 (abstr), 921-922, 1964.

32. Wagner, E., Deutsch Zahnaerztl Z., 17, 99. 1962.

33. Wilkinson, E. G. and Haack, D. C., J. Dent. Res., 37, 136-143. 1958.

34. Young, Franklin A., Jr. and Johnson, Lewis B., Jr., J. Dent. Res., 46, 457. 1967.

35. Young, F. A., Jr. and Wilsdorf, H. G. F., J. Biomed Mat. Res., 6, 81-103. 1972.

University Libraries
University of Missouri

Digitization Information Page

Local identifier	Holland1976

Source information

Format	Book
Content type	Text with images
Source ID	No barcode
Notes	N/A

Capture information

Date captured	12/8/23
Scanner manufacturer	Fujitsu
Scanner model	fi-7460
Scanning system software	ScandAll Pro v. 2.1.5 Premium
Optical resolution	600 dpi
Color settings	8 bit grayscale
File types	tiff
Notes	N/A

Derivatives - Access copy

Compression	Tiff: LZW compression
Editing software	Adobe Photoshop
Resolution	600 dpi
Color	grayscale
File types	tiff
Notes	